Improvements in Design and Manufacturing of Camshafts for High HP Engines

A Dissertation Submitted
In Partial Fulfilment of the Course of

MASTER OF ENGINEERING
in
PRODUCTION ENGINEERING
By

Rajnish Bansal

Under the guidance of:

Dr. Ajay Batish

Professor, MED

Thapar University, Patiala

MECHANICAL ENGINEERING DEPARTMENT

THAPAR UNIVERSITY PATIALA-147004, INDIA

December 2016

DECLARATION

I hereby declare that the thesis titled **'Improvements in Design and Manufacturing of Camshafts for High HP Engines'** is an authentic record of my study carried out as requirement for the award of the degree of **M.E (Production Engineering)**, Mechanical Engineering Department at Thapar University, Patiala under the esteemed supervision of **Dr. Ajay Batish,** Professor, Mechanical Engineering Department, TU during the 4rd semester (Jan–July 2016, extended till Dec'2016). The matter embodied in this report has not been submitted in partial or full to any other university or institute for award of any degree.

Rajnish Bansal
Roll No.801482024

Date: 20.12.2016

It is certified that the above statement made by the student is correct to the best of my knowledge and belief.

Dr. Ajay Batish
Professor
MED, Thapar University
Patiala

Date: 20.12.2016

Countersigned by

Dr. S.K. Mohapatra
Sr. Professor & Head
Mechanical Engineering Department
Thapar University, Patiala-147004

Dr. S.S. Bhatia
Dean of Academic Affairs
Thapar University, Patiala-147004

ACKNOWLEDGEMENTS

I express my deep sense of gratitude and a very sincere thanks to my guide **Dr. Ajay Batish** Professor, Mechanical Engineering Department, Thapar University, Patiala for his inexorable and valuable guidance which helped me in the accomplishment of this present seminar report. I am highly indebted to him for his invaluable suggestions during the period of work.

I also express my gratitude to my better half Anjana for her unrelenting support at this juncture of my life. I am also indebted to Sh. Manoj Kumar, Sr. Section Engineer, CAE at Rail Coach Factory, Kapurthala and Sh. Navdeep Kumar, Sr. Section Engineer, Design, at Diesel Loco Modernisation Works, Patiala for providing me all the support in carrying out Design Analysis of 3-D models. Above all, I express my indebtedness to my parents and the 'ALMIGHTY' for all their blessings.

Rajnish Bansal

ABSTRACT

While designing of components which are required to work under cyclic loading, fatigue life becomes an important parameter. It primarily depends on geometrical features like fillet radius and sharpness of the corners which creates stress concentrations zones. Besides this, surface finish, loading conditions, thermal stresses and metallurgical flaws also play a secondary role. Various studies have been conducted on S-N relationships for simple geometries but in practice these results cannot be used because of dimensional and geometrical constraints imposed by the assembly designs. Nowadays FE analysis is used in such situations. Though it helps in analysing a design but designers need firsthand knowledge about the effect of such constraints on the Stress Concentration to make the design process efficient.

A real life problem faced by Indian Railways on pre-mature fatigue failures of engine camshafts used in upgraded high horsepower diesel locomotives has been taken for study. Reported failures have been analysed and existing design has also been reviewed. Various design options within given constraints have been explored to develop 3-D models on Creo Elements/Pro 5.0 3-D modelling software, followed by meshing on HyperMesh V09 and FE analysis using RADIOSS software. After thorough analysis, the suitability of each options for adoption was adjudged and a combination model was developed to arrive at an optimal solution. A comparative study of different manufacturing processes has also been carried out so that benefits can accrue over and above the improvement made in stress concentration factor by alternate geometry.

The studies conducted through modelling and FEA has revealed that introduction of an undercut groove in the shaft, increase in thickness of the coupling flanges and above all, reduction in the depth of dowel holes can play significant role in reducing the maximum stress induced in the geometries and it can be adopted well in components where there is a space constraint in the assembly and operations. It has also been found that contrary to common belief, blended grooves to increase fillet radius in the flanges increases the induced stress whereas similar grooves in shaft tends to reduce the stress.

Further, the studies made on adopting forging process for manufacturing of camshafts has revealed that not only it helps in improving the mechanical properties significantly, especially

the UTS and Yield Strength at the most vulnerable locations vis-à-vis components manufactured out of round bars, but it also reduces the cost of manufacturing considerably, though it primarily depends on the volume over which cost of forging dies can be amortised. In the current study an improvement of 22% and 26% was achieved in UTS and Yield Strength respectively over the shear plane where failures were occurring along with cost reduction of 21% in the manufacturing cost.

This study can be of great use to designers to understand the effect of variations in common geometrical features on the maximum induced stress while designing various mechanical components transmitting torque. It has a direct correlation with the fatigue life of components during service and thus it can help in improving their reliability. Further, this thesis has established, how forgings can be adopted to strengthen the vulnerable locations and at the same time save upon the cost of manufacturing.

TABLE OF CONTENTS

Declaration …… (i)

Acknowledgements ……... (ii)

Abstract ……. (iii)

Table of contents …….. (v)

List of Figures ……..……. (vii)

List of Tables ……..…….. (xi)

List of Acronyms …….. (xii)

Chapter1 :INTRODUCTION **1–6**

1.1 General…… 1

1.2 The Design and Manufacturing Problem taken up for Study ……..… 4

Chapter 2 : LITERATURE REVIEW **7-14**

2.1 General ……..…… 7

2.2 Summary .....……... 13

2.3 Gaps in research …… 14

2.5 Scope and objective……. 14

Chapter 3 : DESIGN OF THE STUDY **15-23**

3.1 Detailed study of the existing problem…… 15

3.2 Objective & methodology to be adopted ……... 20

3.3 Different options considered for improvement …….. 21

3.4 Design of experiments…… 23

Chapter 4 : EFFECT OF VARIATIONS IN COMPONENT GEOMETRY - BY FEA STUDIES **24-57**

4.1 Study of component geometry and service requirements..... 24

4.2 Study of existing manufacturing process..... 28

4.3 Study of the existing assembly process..... 29

4.4 Different options for changes in geometry..... 30

4.4.1 Effect of undercut radius in the flange on Max. Stress 31

4.4.2 Effect of undercut radius in shaft on max stress 37

4.4.3 Effect of increasing flange thickness of shaft on max stress 42

4.4.4 Effect of reduction in depth of dowel hole on max stress 47

4.4.5 Effect of providing a variable radius 53

4.4.6 Increasing the PCD of coupling holes 53

4.5 Findings and analysis of FEA studies 53

4.6 Development of an optimised model based on FEA studies 53

4.7 Findings and results 57

Chapter 5 : FORGING AS ALTERNATIVE MATERIAL FOR CAMSHAFTS 58

5.1 Introduction..... 58

5.2 Choice of Material..... 59

5.3 Development of forging process for camshafts..... 61

5.4 Validation of results..... 63

5.4.1 Metallurgical Examination 63

5.4.2 Analysis of Grain Flow after Forging 64

5.4.3 Study of physical properties 65

5.4.4 Analysis of Results obtained in Mechanical Testing 71

5.5 Relative economics of adopting forging over rolled bars 72

5.6 Findings and results 74

Chapter 6: FINDINGS AND CONCLUSION 75-77

6.1 Variations between FEA results and actual findings 75

6.2 Validation of results 77

6.3 Scope for further study 77

REFERENCES

LIST OF FIGURES

Fig #	Description of Figure	Page #
1.1	Diesel Electric Locomotives in use on Indian Railways …….....….	1
1.2	General Layout of a Diesel Electric Locomotive …….....……	2
1.3	Modified Indicator Diagram for 3600 HP Upgraded Engines …….....….	3
1.4	Arrangement showing Fuel Injection by Camshaft …….....….	4
1.5	Conventional Camshaft with Base Circle Dia. of 140 mm …….....…..	5
1.6	New Design Stiffer Unit Camshaft with Base Circle Dia of 160 mm ….....……	5
1.7	Engine Block Showing Cam Bores And Front Opening …….....…	5
1.8	Comparison of Old & Modified SUCS (Taper flange vs. Straight flange) ….....	6
2.1	Constant-lifetime Fatigue Diagram for Alloy Steel (TS: 1035 MPa) ……....	8
2.2	Fatigue Life behaviour in Two Different Loading Histories …….....	8
2.3	Test Specimen Designed for Fracture Toughness Studies …….....…	9
2.4	Variation of P_{max} With Notch Root Radius for Different a/W Ratios ….....……	9
2.5	: Variable-Radius Curve …….....……..	10
2.6	Demonstration of Effect of Variable-Radius on Peak Stress ……..... ……	10
2.7	Schematic Representation of Crankshaft and Rolling Process …….....…….	11
2.8	Stress Contour at Fillet …….....…….	11
2.9	Stress field Zones Between 210 MPa to 260 MPa …….....……	12
3.1	Typical Location of Camshaft Flange Breakage Due to Fatigue ….....…….	16
3.2	Fracture Pattern as Observed on Failed Camshafts …….....……..	17
3.3	Microstructure as Observed on Failed Camshafts (100X) …….....……	17
3.4	Section of Camshaft Segment …….……..	19

Fig #	Description of Figure	Page #
3.5	Proposed Increase in Fillet Radius …….……	21
3.6	Dowel Hole for Depth Optimization …….....…….	21
3.7	Undercut Root Radius ……	22
3.8	Optimization of Variable-Root Radius ……..	22
3.9	8-Hole Configuration With More PCD …….....…….	22
3.10	Comparison of Grain Structure in a) Forging b) Machining c) Casting ….....…....	23
4.1	Arrangement showing the coupling and coupling screw resisting the torque.....	26
4.2	Meshing done using HyperMesh v09 Software using Tetrahedral elements of 2mm size	27
4.3	Model with tangential force component in meshed condition	27
4.4	FEA of the model showing Max Stress (Von Mises)	27
4.5	3-D Model depicting undercut groove in the flange at the location of stress concentration zone	31
4.6	Meshing done on HyperMesh v09 Software using Tetrahedral elements of 2mm size with undercut in flange	34
4.7	Conversion of torque into equivalent force elements applied at PCD before FEA (with undercut in flange)	34
4.8	FEA of the meshed model with undercut radius 2.16 mm on RADIOSS solver	35
4.9	FEA of the meshed model with undercut radius 2.54 mm on RADIOSS solver	35
4.10	FEA of the meshed model with undercut radius 2.92 mm on RADIOSS solver	35
4.11	Plot showing variation in Max Stress (Von Mises) w.r.t. undercut radius in flange	36
4.12	3-D Model depicting undercut radius in the shaft at the location of stress concentration zone	37
4.13	Meshing done on HyperMesh v09 Software using Tetrahedral elements of 2mm size	39
4.14	Conversion of torque into equivalent force elements applied at PCD before FEA	40
4.15	FEA of the meshed model with undercut radius 2.92 mm on RADIOSS solver	40

Fig #	Description of Figure	Page #
4.16	Plot showing variation in Max Stress (Von Mises) w.r.t. undercut radius in shaft	41
4.17	3-D Model depicting flange width near stress concentration zone	42
4.18	Meshing done on Hypermesh v09 Software using Tetrahedral elements of 2mm size	44
4.19	Conversion of torque into equivalent force elements applied at PCD before FEA	45
4.20	FEA of the meshed model with increased flange thickness of 26.99 mm on RADIOSS solver	45
4.21	Plot showing variation in Max Stress (Von Mises) w.r.t. increase in flange thickness	46
4.22	3-D Model depicting dowel hole depth near stress concentration zone	47
4.23	Meshing done on Hypermesh v09 Software using Tetrahedral elements of 2mm size	50
4.24	Conversion of torque into equivalent force elements applied at PCD before FEA	50
4.25	FEA of the meshed model with dowel hole depth of 12.7 mm on RADIOSS solver	51
4.26	FEA of the meshed model with dowel hole depth of 7.62 mm on RADIOSS solver	51
4.27	Plot showing variation in Max Stress (Von Mises) w.r.t. decrease in Dowel Hole Depth	52
4.28	Optimised 3-D Model with undercut radius of 3.05 mm, flange thickness of 26.99 mm & reduced depth of dowel hole of 7.62 mm	54
4.29	Meshing done on HyperMesh v09 Software using Tetrahedral elements of 2mm size	56
4.30	Conversion of torque into equivalent force elements applied at PCD before FEA	56
4.31	FEA of the Optimised 3-D Model with undercut radius of 3.05 mm, flange thickness of 26.99 mm & reduced depth of dowel hole of 7.62 mm on RADIOSS solver	57
5.1	Steps showing simulation of Stiffer Unit Camshaft Segment Die Forging, run on FORGE ® NxT Ver. 3.0 Software	62
5.2	Digital Microscope used for metallurgical examination…….	63
5.3	Comparison of Micro Structure observed at 100 X – There is grain refinement after forging	63

Fig #	Description of Figure	Page #
5.4	Grain flow lines as observed in a cut section of the forging ……	64
5.5	Scheme of samples prepared for study of Mechanical Properties in three different directions	65
5.6	Location and alignment, from where sample is drwan for evaluating the Mechanical Properties of the Forging	66
5.7	Computerised Universal Testing Machine, Model TUE-C-400 available in the DMW Laboratory used for testing of Mechanical Properties of the samples	66
5.8	One of the test specimen showing cup and cone type breakage ……	71
5.9	A proof machined forging adopted for manufacturing of Stiffer Unit Camshafts	72

LIST OF TABLES

Fig #	Description of figure	Page #
3.1	Duty Cycle of Locomotives ……..…….	15
3. 2	Failures reported on Stiffer Unit Camshafts …….....…….....	16
3.3	Chemical Properties of AISI E 1070 Steel …….....……	18
4.1	Three proposed models with variations in undercut radius in flange	32
4.2	Results obtained from FEA by introducing undercut radius in the flange	36
4.3	Three proposed models with variations in undercut radius in shaft	38
4.4	Results obtained from FEA by introducing undercut radius in the shaft	40
4.5	Three proposed models with variations in undercut radius in shaft	43
4.6	Results obtained from FEA by increasing flange thickness	46
4.7	Three proposed models with variations in dowel hole depth	48
4.8	Results obtained from FEA by increasing flange thickness	52
5.1	Mechanical Properties of Magnaflux Quality AISI E 1070 Grade Hot Rolled, Normalized and Tempered Steel suitable for Induction Hardening	59
5.2	Chemical Properties of Magnaflux Quality AISI E 1070 Grade Hot Rolled, Normalized and Tempered Steel suitable for Induction Hardening	60
5.3	Mechanical Properties of Round Bar AISI E 1070 Steel (Along Grain Flow)	67
5.4	Mechanical Properties of Round Bar AISI E 1070 Steel (Across Grain Flow)	68
5.5	Mechanical Properties of Round Bar AISI E 1070 Steel (At 45° plane)	69
5.6	Mechanical Properties of Forging AISI E 1070 Steel (At 45° plane)	70
5.7	Comparison of Mechanical Properties of Forged component over Round Bar at 45° shear plane	71
5.8	A comparison of stock removed in machining in the two processes	72
5.9	Table showing cost comparison of the two processes; Round Bar Vs Forging	73

LIST OF ACRONYMS AND ABBREVIATIONS

ABB	Asean Brown & Boweri Ltd.
ALCO	American Locomotive Company, USA
AISI	American Iron and Steel Institute
ASTM	American Society for Testing of Materials
bTDC	Before Top Dead Centre
BHN	Brinell Hardness
CAGR	Compounded Annual Growth Rate
DMW	Diesel Loco Modernisation Works, Patiala
EMD	Electro-Motive Division (Erstwhile group company of General Motors Inc.)
FEA	Finite Element Analysis
HP	Horsepower
H_v	Vicker's Hardness
K_f	Fatigue Notch Factor
IR	Indian Railways
MPa	Mega Pascal
P-V	Pressure-Volume
PCD	Pitch Circle Diameter
SCF, K_t	Stress Concentration Factor
SUCS	Stiffer Unit Camshaft
T_{max}	Maximum Torque
τ_{max}	Max. Shear Stress
UTS	Ultimate Tensile Strength
VHCF	Very High Cycle Frequency

CHAPTER 1

INTRODUCTION

1.1 GENERAL

Traffic on Indian Railways is growing at a CAGR of 8%, however there has been limited growth of rail network due to its capital intensiveness. Limited network is putting heavy burden on the system to cater to the increase in traffic and as a result, lot of traffic is moving to roads even when it is uneconomical.

Increasing number of trains on the already clogged network is almost impossible. In this situation IR has adopted a policy of running longer trains without loss of speed. This approach however requires higher horse power locomotives. Thus IR bought technology from international players like ABB and EMD for producing locomotives of power rating 4000 HP or higher. But at the same time, it has a fleet of almost 6000 locomotives which are rated below 3000 HP and still has an average residual life of more than 20 years.

2600 HP WDM_2
ALCO Locomotives
(16 Cylinder V Engines)

4500-5500 HP $WDG_{4/5}$
EMD Locomotives
(20/24 Cylinder V- Engines

Fig:1.1 Diesel Electric Locomotives in use on Indian Railways

Predominantly it is the WDM_2 series of ALCO locomotives that have been the workhorse of Indian Railways since 1960s. These locomotives were equipped with 2600 HP 16-cylinder turbocharged V-engines. So a decision was taken to upgrade these locomotives to higher HP to match the ever increasing demand.

Indian Railways had set up a fully owned unit called Diesel Loco Modernisation Works at Patiala, where mid-life rehabilitation of WDM_2 is carried out once they complete half of their expected life of 36 years. During Rehab, some other technology enhancing upgrades are also applied. So in addition power upgrade was also planned and for this, technology was developed by Railway's R&D wing, Engine Development Directorate of Research Design & Standards Organisation (RDSO), Lucknow in association with General Electric Transportation Systems Ltd., India.

During mid-life Rehab, DMW had been continuously upgrading these locomotives in terms of higher fuel efficiency, transmission systems and reduced maintenance frequency. Now a major **Retro-Upgrade** is applied to these locomotives during their mid-life rehab (after 18 years of service), that includes;

1. Increasing the engine horse power from 2600 HP to 3300/3600 HP
2. Switching over from conventional DC-DC transmission to AC-DC transmission
3. Micro-processor based fuel governing system replacing electro-hydraulic governors
4. Micro-processor based propulsion control system
5. Upgrading systems for increasing maintenance frequency from 7 days to 30 days.

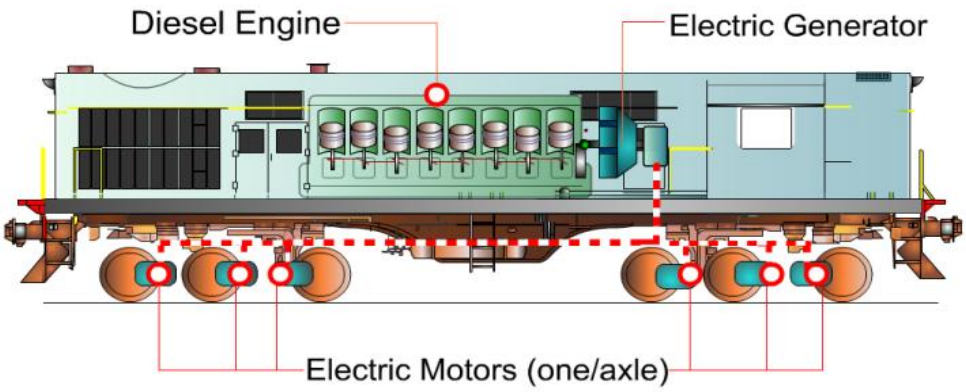

Fig:1.2 General Layout of a Diesel Electric Locomotive [11]

Of these, increasing engine horse power by about 40% using the same engine block is a major challenge. This has been achieved by applying a technology upgrade to many parts of the engine. The changes made to design of engines included;

a. Increasing peak speed from 1000 RPM to 1100 RPM

b. Increasing Booster Air Pressure from 1.8 kgf/cm^2 to 2.2 kgf/cm^2

(achieved by higher efficiency turbo chargers – 70% and larger after cooler)

c. Use of super bowl pistons with higher compression ratio (11.75)

d. Modified cylinder heads with streamlined air flow and better cooling

e. And most importantly it is redefining the P-V diagram wherein peak firing pressures have been reduced while increasing the Mean Effective Pressure in the engine. It has been accomplished by delaying the fuel injection (from 25.5 º bTDC to 22° bTDC) and injecting it at higher air compression pressures. As a result, combustion is delayed and peak firing pressures are reduced because by that time return stroke (power delivery stroke) of piston starts. But at the same time power, is delivered for a longer duration and at higher mean pressures.

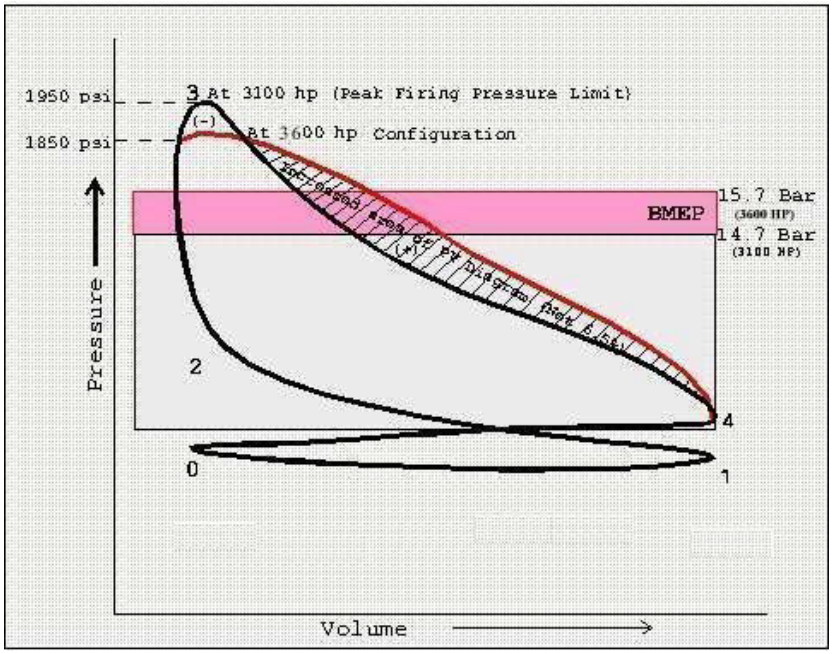

Fig:1.3 Modified Indicator Diagram for 3600 HP Upgraded Engines [11]

This design change has led to series of other design changes in the engine components where stress levels have increased.

1.2 DESIGN AND MANUFACTURING PROBLEM TAKEN UP FOR STUDY

As mentioned in Para 1.1 above, the modified Indicator diagram warranted fuel injection at much higher injection pressure. It went up from 750 bars to 1100 bars. This additional pressure is to be withstood by the camshaft as shown in the picture below.

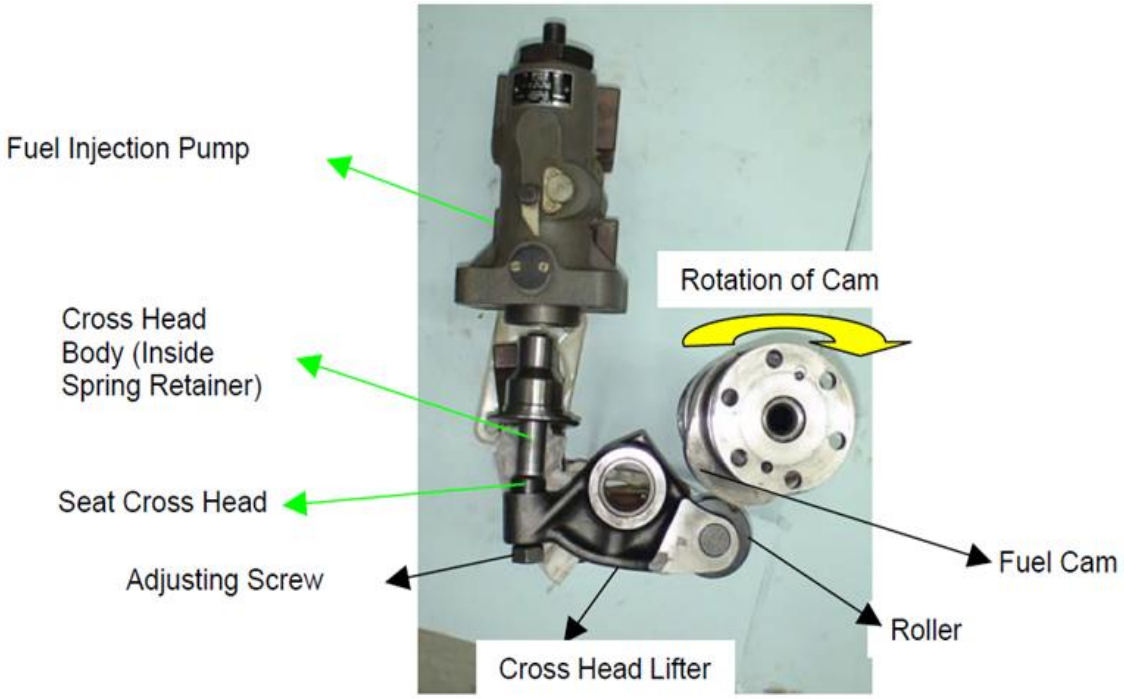

Fig1.4: Arrangement showing Fuel Injection by Camshaft [(11)]

So a totally new design of cam shaft was required. The most significant being, redesigning of the camshaft and its lobes so as to withstand higher compression pressures during fuel injection. Following constraints were put on the designing of camshaft;

1. There should be the minimum or no modifications to the engine block which meant that the cam bores in the engine block are not to be disturbed as it required cutting of critical section of the block and welding new cam bore housings resulting in thermal distortions in the engine block.
2. Fitment of modified camshaft should not pose any problem for which either side insertion can be used as in the existing camshafts or front window in the engine block can be used for direct insertion.
3. Materials selected should be such that these are available in Indian Market and their hardenability by induction hardening process does not pose any problem. Manufacturability of camshaft.
4. Replacement of camshafts should not pose any problem during field service.

Within these constraints, a new design was developed and it served most of the needs.

1. The new design has a base circle diameter of 160 mm instead of 140 mm of earlier design. This necessitated insertion of camshaft only from the front window of the block as the dia was bigger than cam bore.

Fig:1.5 Conventional Camshaft with Base Circle Dia of 140 mm [11]

Fig: 1.6 New Design Stiffer Unit Camshaft with Base Circle Dia of 160 mm [11]

2. The new design also offered the advantage of variety reduction as only one common design was adopted for all camshafts with different in bearing pieces. Most of the wear takes place at cam lobes, so only cam segments could be replaced.

3. It is possible to insert it from front window so time for replacement could be considerably reduced, thus reducing the loco downtime in the event of camshaft replacements in field service or during periodic maintenance.

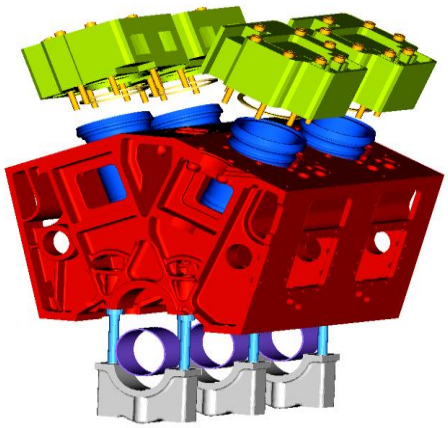

Fig: 1.7 Engine Block Showing Cam Bores and Front Opening [12]

The new design posed a serious problem in manufacturing as drilling of coupling holes on taper portion followed by making of a counter sunk seat for the allen head screws was quite cumbersome and highly time consuming. To eliminate this process, a straight flange was adopted instead. However its flange thickness was increased to compensate for strength.

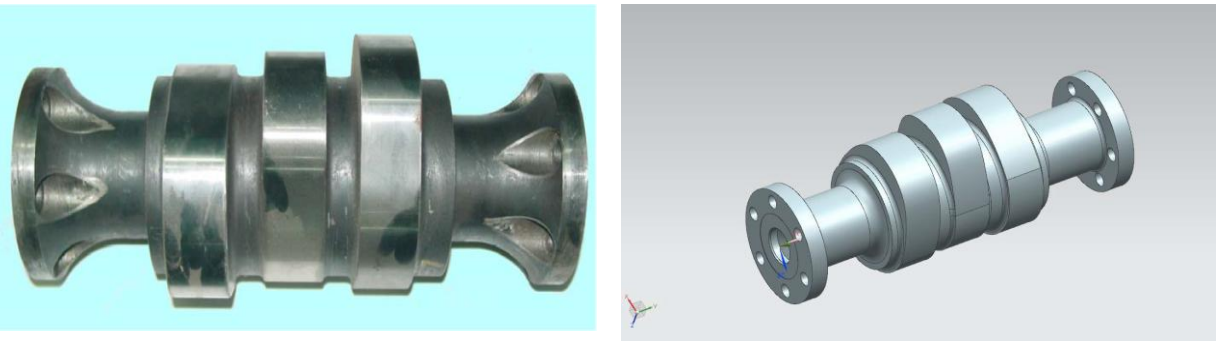

SUCS with taper flange/counter sunk holes SUCS with straight flange

Fig:1.8 Comparison of Old & Modified SUCS (Taper flange vs. Straight flange)[20]

Though it simplified the manufacturing process, but during service, flange breakage cases are being reported in many locomotives posing a serious reliability problem.

No proper solution could be found to this problem and it could have jeopardised the ambitious locomotive upgradation project. Diesel Loco Sheds have been resorting to downgrading these locomotives in service so as to improve their reliability at the cost of higher power.

This problem has been taken up as a project for the study and to find an optimal solution has been made its objective. The new learnings made in the process have been made the basis for this dissertation.

Chapter 2

LITERATURE REVIEW

2.1 GENERAL

A well defined problem is at hand, thus a focused search for available technical literature has been made so that all related aspects can be examined and a problem is found to the solution. If a readymade solution is not found then the knowledge gathered during the process is used to find the gaps and further research is carried out in a chosen area which should not only help solving the existing problem but act as a knowledge base for handling similar situations.

Here the problem is specific but still it is quite common in the industry where shafts used for torque transmission under cyclic loads fail pre-maturely in service. In similar situations, designers do not have a clear understanding of the causes of failures and standard deign handbooks are not able to resolve the mystery behind fatigue failures.

Fortunately, Finite Element Analysis tools available today are quite helpful in handling complicated designs, but it is not easy to deploy them in all situations. Moreover it is important to know, what factors have significant impact on the Stress Concentration Factor in similar geometries and how can these be resolved.

Literature review with these points under consideration has resulted in quite an interesting findings which are summarised here.

2.1.1 Boardman, in his paper titled "***Fatigue Resistance of Steels****" [1990]* [(1)] presented a comprehensive study on fatigue behaviour of steel which was adopted as a part of ASTM handbook on Properties and Selection: Irons, Steels, and High-Performance Alloys. He emphasized that fatigue cracks are progressive and follows a step by step phenomenon. Initially a fatigue damage leads to crack initiation then the Crack propagates to some critical size at which the remaining un-cracked cross section of the part becomes too weak to carry the imposed loads and it fails suddenly. Fatigue strength not only depends upon the UTS of material but also on metallurgical flaws, surface finish, component geometry and service conditions (Loading/Un-loading cycles) etc.

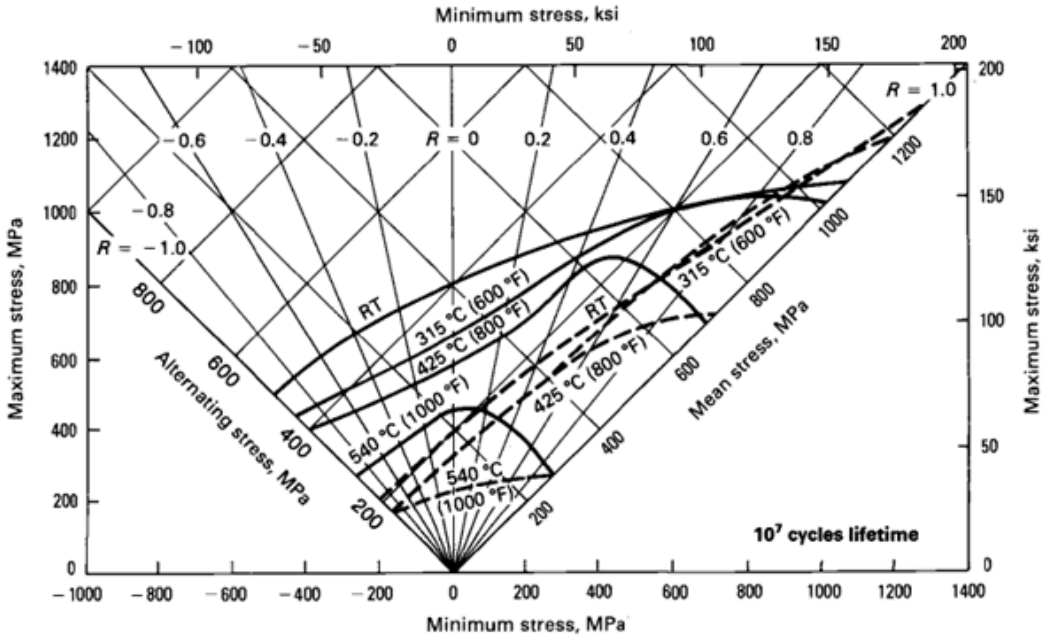

Fig: 2.1 Constant-lifetime Fatigue Diagram for Alloy Steel (UTS: 1035 MPa) [1]

#Solid lines- Unnotched, Dashed Lines- Notched Specimens, in 10^7 cycles

The above plot shows the dependence of fatigue life on Max Stress, Minimum Stress, Alternating Stress and Stress Ratio.

He found another interesting phenomenon in which loading history also plays a significant role in deciding fatigue life. Two stress histories are shown in situation A & B. It was found that fatigue life was less in case A compared to B.

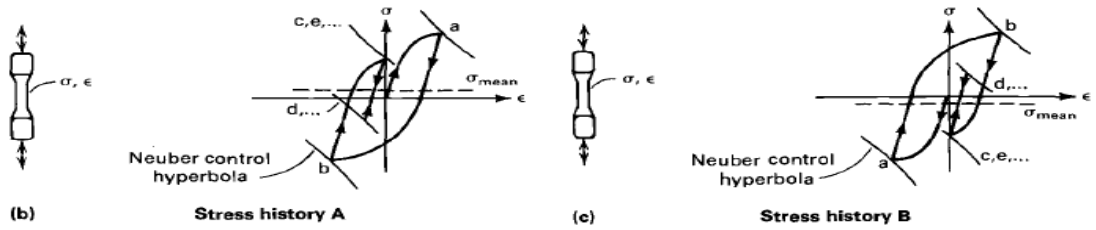

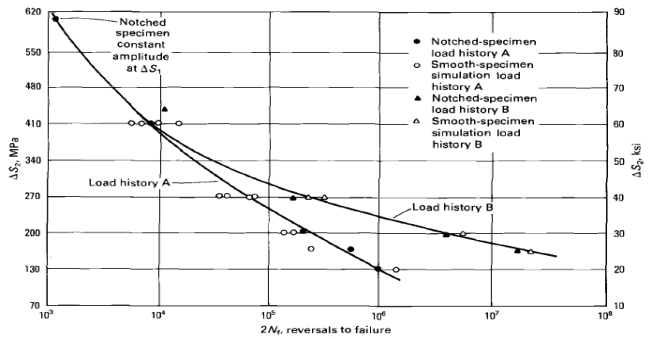

Fig:2.2 Fatigue Life behaviour in Two Different Loading Histories[1]

***2.1.2 Mourad** et.al.* in their paper titled *" **Fracture toughness prediction of low alloy steel as a function of specimen notch root radius and size constraints*"** [2013] [(2)] presented a model for predicting fracture toughness in notched geometries.

His studies were based on a test specimen as shown in the figure below.

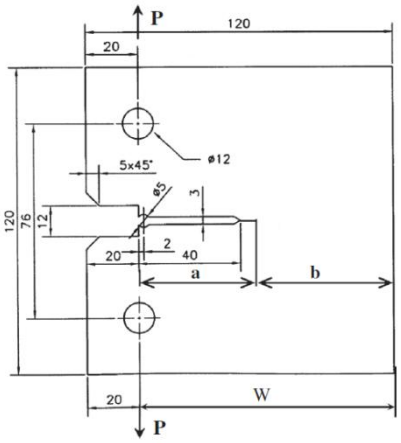

Fig:2.3 Test Specimen Designed for Fracture Toughness Studies [(2)]

In his studies, he established that fracture toughness is function of both notch root radius and a/W ratio but notch depth plays more significant role as compared to the notch radius. A critical notch root radius was found at which the fracture toughness is completely independent of the notch root radius for all specimens with different ligament lengths. Empirical formula derived from the studies can be used for finding critical notch root radius for better designs.

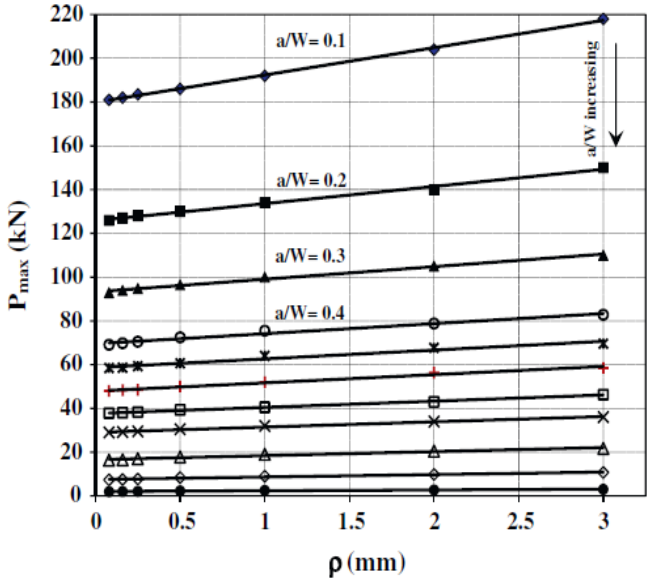

Fig:2.4 Variation of P_{max} With Notch Root Radius for Different a/W Ratios [(2)]

***2.1.3 Taylor** et.al.* in their paper titled *"**The variable-radius notch: Two new methods for reducing stress concentration**"* [2011] [3] presented an interesting finding that instead of a constant radius fillet, variable-radius fillets can be made which can significantly reduce the stress concentration factors at fillets.

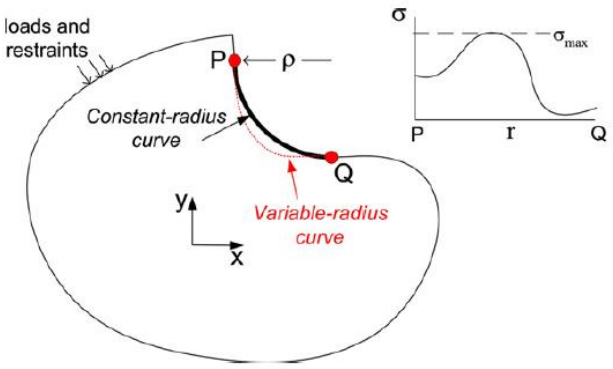

Fig:2.5 Variable-Radius Curve [3]

Their theory is based on the pretext that in cyclic loading, the load varies as a function of radius. Therefore fillet radius can be made variable depending upon the load distribution over a cycle. It is demonstrated in their FEM Analysis of a sample case as shown below;

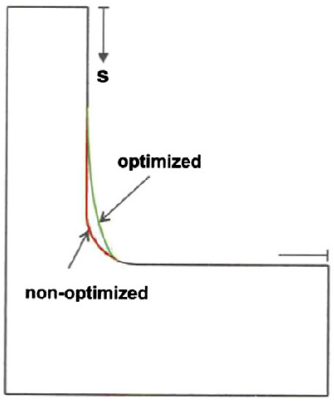

Peak Stress level in optimized radius could be brought down from 214 MPa to 122 MPa

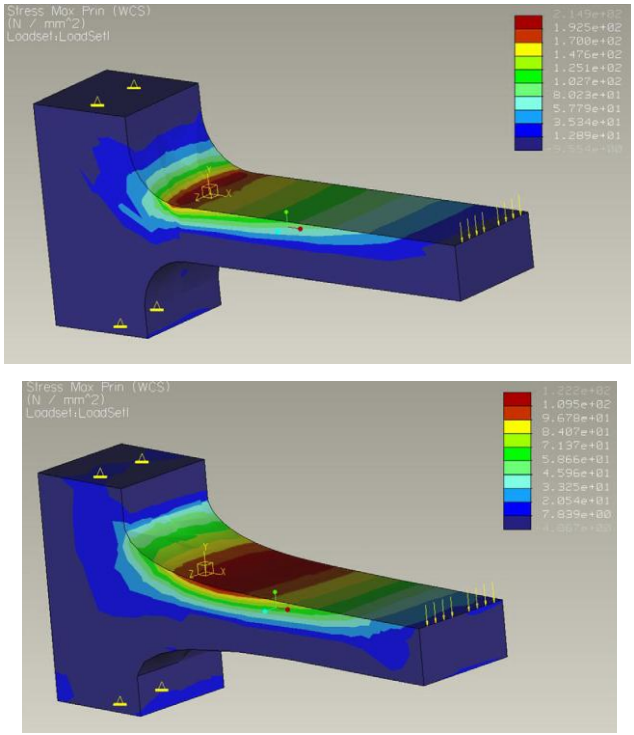

Fig:2.6 Demonstration of Effect of Variable-Radius on Peak Stress [3]

They also developed a simple method to evaluate the radius in simple situations, however FE Analysis technique was recommnded for complex geometries and loading patterns.

***2.1.4 Cevik** et.al.* in their paper titled *"**The Evaluation of fatigue performance of a fillet rolled diesel engine crankshaft**"* [2013] [(4)] came out with novel technique to reduce stress concentration factor using rolling process for making fillets. The results obtained were extra-ordinary because the Stress Concentration Factor could be reduced to one-fourth its original value.

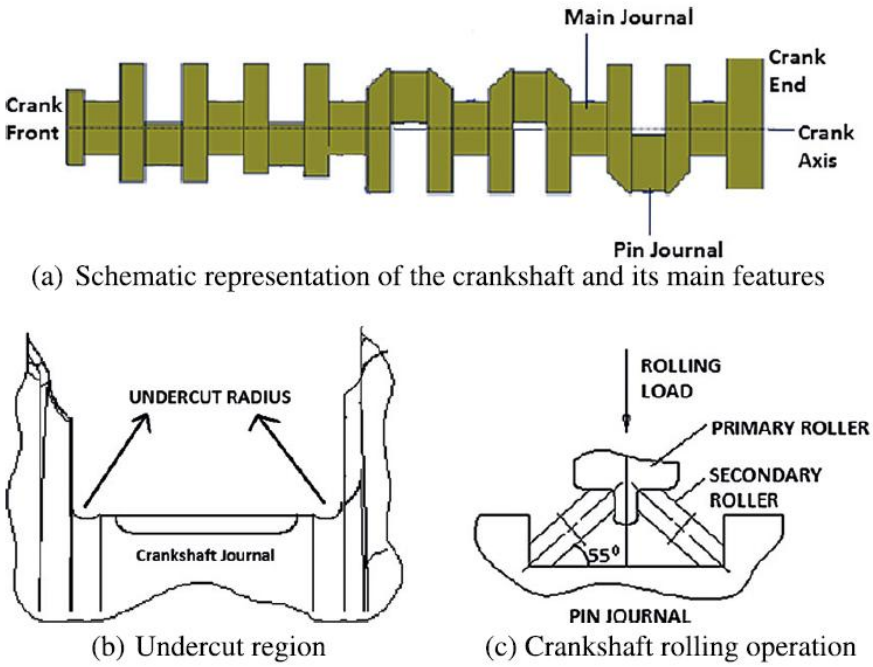

Fig:2.7 Schematic Representation of Crankshaft and Rolling Process [(4)]

Further in order to expedite testing of endurance limit, they used staircase test methodology. Experimental results showed that mean fatigue limit could be raised from 201 MPa in case of un-rolled fillet to 841 MPa for rolled fillet. Thus it presents a strong case for adopting rolling process for fillets in critically stressed section with cyclic loading. It can find good use for crankshafts, camshafts and other similar components.

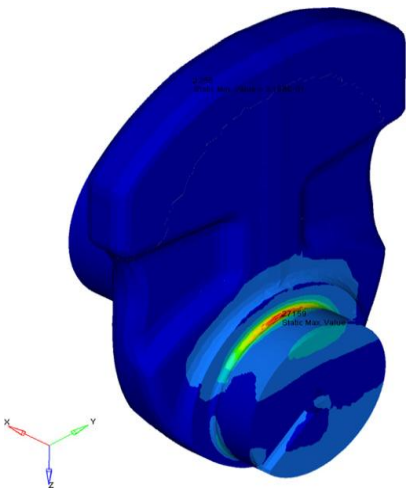

Fig:2.8 Stress Contour at Fillet [(4)]

2.1.5 Bandara *et.al.* in their paper titled *"**Fatigue failure predictions for steels in the very high cycle region – A review and recommendations***"* [2014] [(5)] came out with a finding that fatigue failures beyond 10^7 cycles (in VHCF) can be due to presence of flaws thus there is no fatigue limit or endurance limit for steels against earlier assumptions. The flaw acts as a fatigue nucleus and it grows to a critical size proportional to square root of area. Once this growth happens, fatigue crack originates and propagates leading to a failure.

It is impossible to measure the size of this area but it has been statistically calculated to be around 24.3 micro meters. The problem was that it could not be related to physically properties of the material. But in these studies, an empirical relationship has been established where UTS and Vickers Hardness Hv can be used to predict the size of this inclusion. Which can further be used for finding endurance limit of a steel. The empirical formula is given below;

$$\sigma_w = (155 - 7\log N) \cdot \frac{(Hv + 120)}{1000} (\sigma_u)^{1/3} \left(\frac{1-R}{2}\right)^{\alpha}$$

2.1.6 Espadafor *et.al.* in their paper titled *"**Analysis of a diesel generator crankshaft failure**"* [2009] [(6)] analysed failure of crankshaft used for 1.5 MW power plant. The failure was analysed by carrying out an FEM analysis of load distribution on the crankshaft. The areas which were most critically stressed as per FEM analysis were actually found to be the region where fatigue failure had originated. A thin and very hard zone was also discovered in the template surface close to the fracture initiation point, which suggests that this was the origin of the fatigue fracture.

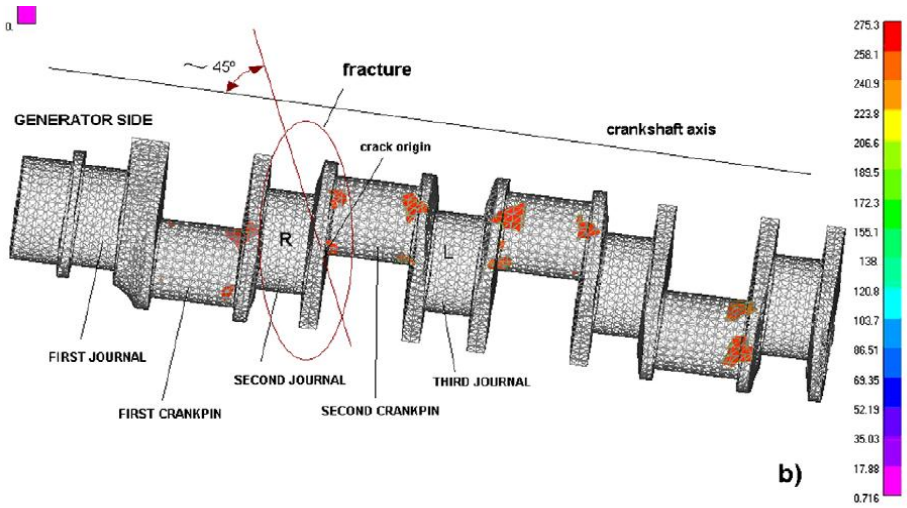

Fig:2.9 Stress field Zones Between 210 MPa to 260 MPa [(5)]

This study is a validation of the fact that the most stressed zone will have maximum chances of fatigue failures, thus designers should analyse their design for maximum stress concentration zones and try to modify their designs to have an even distribution of stress in critical zones.

2.2 SUMMARY

Following can be summarised from the literature survey;

2.2.1 From the literature survey, it has been found that there are very limited studies available on analysis of fatigue failures. However efforts have been made to find out different methods to minimize Stress Concentration Factor K_t which is the ratio of max stress to the nominal stress and it plays most significant role in fatigue failures.

2.2.2 Besides this, in case of notched geometries it gets modified to Fatigue Notch Factor K_f which is a ratio of Smooth fatigue strength to Notched fatigue strength. Accordingly a term called notch sensitivity has been defined which relates these two factors.

2.2.3 Stress gradient is also important because the notch stress controlling the fatigue life is not the maximum stress on the surface of the notch root, but an average stress acting over a finite volume of the material at the notch root. This avg. stress is lower than the max. surface stress, calculated from K_t.

2.2.4 Sequence of loading also plays significant effect in the fatigue life of steels.

2.2.5 Steels have no fatigue limits. Fatigue failures also occur beyond 10^7 cycles due to inclusions which once grow beyond critical size and it can be predicted by strength parameters σ_u (UTS) and H_v (Vicker's Hardness).

2.2.6 K_t factors can be considerably reduced by adopting variable-radius notches in comparison to constant radius notches. This is because in cyclic loading, the load varies as a function of radius.

2.2.7 By using rolling instead of turning for making fillets on crankshaft, four-fold increase could be achieved in endurance limit of steel.

2.3 GAPS IN RESEARCH

2.3.1 **Stress concentration factors** have been calculated by different methods, like mathematical equations, empirical relations and by Finite Element Analysis. Available studies are for simple designs and shapes but no literature could be found on the **effects of other geometrical constraints** like tubular structures and flanged couplings etc. especially under **Torsion**.

2.3.2 No study is available on effect of using **variable radius fillets under Torsion Loads on stepped shafts.**

2.3.3 Effect of **undercut fillets vis-à-vis normal fillet radius** on SCF has not been examined.

2.3.4 **Forged steel** with specific direction of grain flow can reduce SCF, but no such studies could be found.

2.5 SCOPE AND OBJECTIVE

The Study is intended **to** minimize the **Stress Concentration Factor** for coupled flanged joints of stepped/notched shafts under **Torsion.** This is with an aim to find a lasting solution to the problem faced by Indian Railways on their upgraded engines. After finding gaps in research it has been decided to examine the effect of following parameters on Stress Concentration Factor and find an optimal solution.

1. Fillet Radius (External radius and Undercut radius)
2. Variable radius fillets
3. Variation in flange thickness
4. Effect of increase and decrease in number of coupling holes
5. Effect of other weakening geometries like dowel hole etc.

After the studies are made, it is proposed to apply the results to the camshaft design problem and validate the findings.

Chapter 3

DESIGN OF THE STUDY

3.1 DETAILED STUDY OF THE EXISTING PROBLEM

Before a formal study is designed, it is imperative that all aspects of the existing problem at hand are studied. So a comprehensive study has been conducted to see various aspects of the problem.

3.1.1 STUDY OF FAILURES (INVESTIGATIONS)

Though many failures have been reported on Stiffer Unit Camshafts as mentioned in Chapter1 but few representative cases have been picked for detailed study.

Estimation of no. of cycles to failure

A locomotive working on Indian Railways undergoes a typical duty cycle as tabulated below;

Table: 3.1 Duty Cycle of Locomotives [21]

Notch	8	7	6	5	4	3	2	1	Idle
RPM	1100	980	860	740	640	580	510	450	350
Duty Cycle %age									
Passenger Service	22	6	4	8	4	8	5	6	38
Freight Service	22	7	5	3.5	3.5	3.5	3	1.5	51

The type of locomotives under study are mixed use locos means they serve both passenger as well as freight services with a ratio of 1:2 approximately so weighted average has been taken to calculate number of cycles the engine and the camshafts may undergo per month.

Also it has been presumed that a locomotive remains in service for about 18 hrs. a day (Based on Indian Railway Year Book (2013-14).

It comes out to be 6,83,000 cycles per day of engine. Camshaft rotates at half the RPM of engine crankshaft, therefore no. of cycles of camshaft can be taken about 3,42,000 per day and this translates to 1.02×10^7 cycles per month.

A summary of failures taken for study is tabulated and their cycles prior to failures are estimated based on above figures. As can be seen that failures have occurred in a wide range of time ranging between 8 months to 33 months of service, but it falls much shorter than the

reliable life of minimum 72 months when a locomotives undergoes a major overhaul and a new set of camshafts is fitted irrespective of the condition of the existing set as a measure of preventive maintenance.

Summary of failures and cycles before failure are tabulated below;

Table: 3.2 Failures reported on Stiffer Unit Camshafts [21]

Loco No.	Date Fitment	Date Failure	Months to Failure	Approx. no. of cycles (10^8)
11242	31-10-2013	07-07-2014	8	0.81
11243	25-09-2013	24-05-2015	20	2.04
13638	02-04-2013	11-10-2014	19	1.94
16349	01-07-2014	15-05-2015	11	1.12
11397	01-12-2012	17-08-2015	33	3.37
13176	01-12-2013	13-05-2015	18	1.84

Data shows that most of the failures are in the range of $\mathbf{10^8}$ cycles.

Metallurgical Investigations:

Metallurgical examination reports of these failures have also been obtained.

The pattern of failure is similar in all the cases.

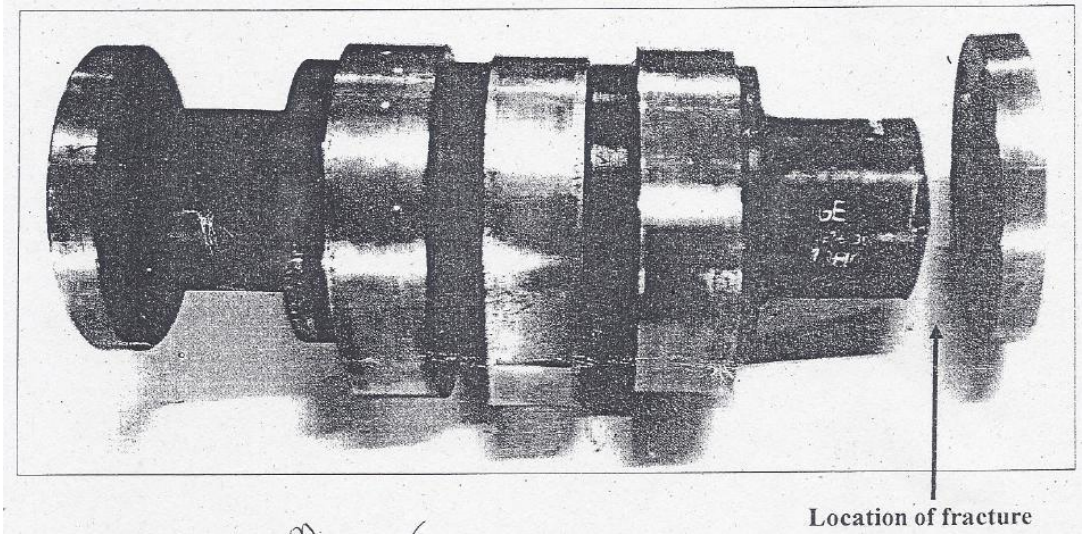

Fig:3.1 Typical Location of Camshaft Flange Breakage Due to Fatigue [21]

It has also been seen from the reports that the failure is on those camshaft segments which are closer to the camshaft drive gear. So it is in direct consonance with the torque and level of stress which is the maximum in those locations compared to camshaft segments on the farther cylinders.

The failed segments have been pictured by respective maintenance sheds and the photographs made available are presented here.

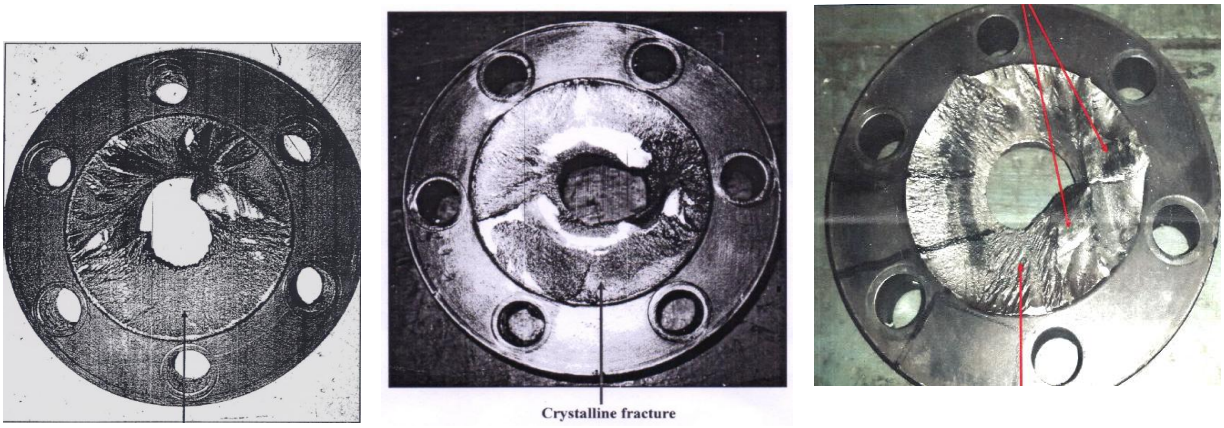

Loco No. 11242 Loco No. 11243 Loco No. 13638

Fig:3.2 Fracture Pattern as Observed on Failed Camshafts [21]

It is observed that failure pattern is identical in all cases and it is originating in the vicinity of dowel hole. It indicates that zone near dowel hole is most critical and stresses developed are highest in the region. However it needs to be examined by design calculations.

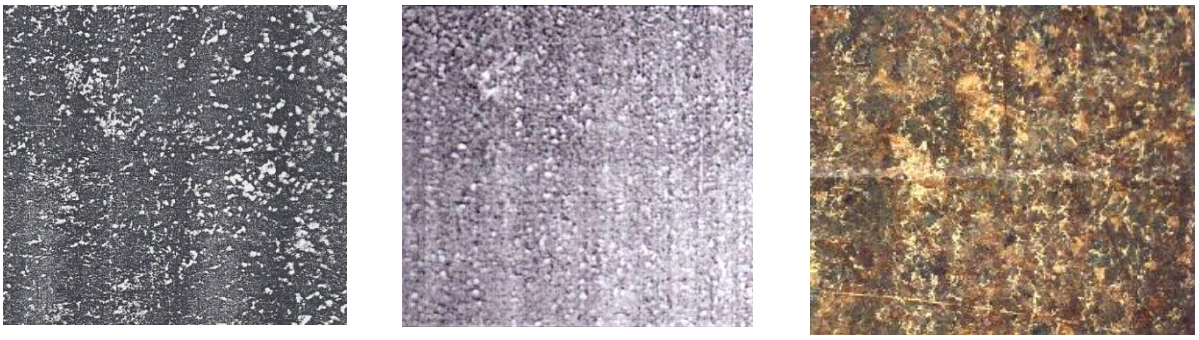

Loco No. 11242 Loco No. 11243 Loco No. 13638

Fig:3.3 Microstructure as Observed on Failed Camshafts (100X) [21]

The pattern observed has been found to be of a matrix of Ferrite and Pearlite grains of ASTM No. 6 which are as per design specification of the material. Inclusion of Type-A 0.5 Thin have been observed in all cases which within specified range of Type-A,B,C,D 0.5 Thick and upto 1.0 Thin.

Conclusion: Therefore no severe irregularity has been observed in the micro structure of failed camshafts which could be attributed to the cause of failure. All these failures have been attributed to sudden change in section leading to fatigue failures.

3.1.2 REVIEW OF EXISTING DESIGN

As the metallurgical investigations have pointed out towards sudden change in the cross section of the camshaft segments as a primary cause of the failure, it was felt necessary that the design of the existing camshaft should be reviewed for it endurance strength with the given geometry.

Design Calculations of Existing Design

The material being used for manufacture of camshafts is equivalent of AISI E 1070 (Magnaflux quality) which has following mechanical and chemical properties;

Chemical Properties

Table 3.3 : Chemical Properties of AISI E 1070 Steel [20]

Sr.	Constituent	Range
1	Carbon	0.65 -0.75 %
2	Manganese	0.5 -0.8 %
3	Phosphorus	0.03% Max
4	Sulphur	0.03% Max

Mechanical Properties:

The steel is procured in rolled bars of 160 mm dia in annealed condition and it is turned to shape on CNC turning centers. In the annealed condition, it possesses following mechanical properties;

Tensile strength : 640 MPa
Shear strength : 320 MPa
Elastic Modulus = (Tensile stress/strain) 190 -210 GPa
Poisson's ratio : 0.25 – 0.3

Moreover, the fatigue strength of stepped camshaft will depend upon the its geometry so relevant dimensions have been chosen for review.

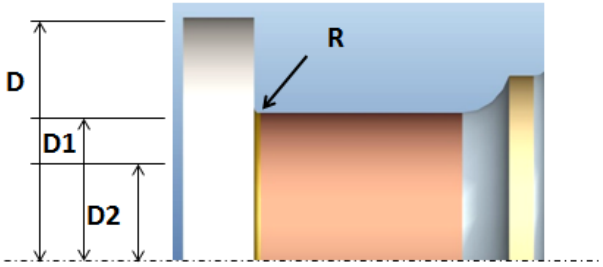

Fig: 3.4 Section of Camshaft Segment

Design Parameters

Max Torque T_{max} = 1996 Nm (2000 Nm)

D = 119.1 mm

D_1 = 59.92 mm

D_2 =19.05 mm

R = 3.175 mm

Calculations:

Endurance Limit for shear = Shear strength x Endurance Factor (E_f)

= 320 MPa X **0.46** = 147 MPa

(E_f value taken from standard tables for normalised high carbon steel)

Polar Moment of Inertia J = pi x (D_1^2-D_2^2) /32 = 1.2504 x 10^{-6} m^4

Max. Shear Stress τ_{max} = T_{max} x D_1 / 2J

= 95.7 MPa

Due to sudden decrease in section, a Stress Concentration Factor (K_t) needs to applied. It is based on following geometrical parameters

1. R/D1 = .053
2. D/D1 = 1.99

From design handbook, the value of Stress Concentration Factor (K_t) = 1.75

Therefore Max shear stress with K_t τ_{kt} = 95.7 MPa x 1.75

= 167.42 MPa

Conclusions:

1. These simple calculations reveals that in the existing design, Max. Shear Stress is more than endurance limit of the steel used for the application.

2. Therefore, the design needs to be reviewed so that stress concentration factor (K_t) can be reduced well below 1.5, so as to factor in Surface finish and Metallurgical irregularities also and obtain a desired fatigue life.

3. The simplest would have been to increase the fillet radius to above 8 mm but geometrical and manufacturing constraints does not warrant such a change.

4. This also indicates that we should look for avenues not only in geometry but also in choice of materials and the manufacturing process to resolve the issue.

5. A detailed literature survey on the subject can be put to use for finding other alternatives which are superior in both technical and economical points of view.

3.2 OBJECTIVE & METHODOLOGY TO BE ADOPTED

At this stage it is felt that following methodology should be adopted to find a solution to the problem and the learning made in the process is presented as a part of the dissertation.

1. Study available technical literature in related fields
2. Carry out 3-D modelling of different sizes and shapes.
3. Carry out optimization of design (Reduction in Stress Concentration Factor) using FE Analysis for different shapes and sizes. It is proposed to use 'HyperMesh' software for meshing and RADIOSS as solver for the FE analysis.
4. Depending upon no. of parameters a suitable model like L-9 of Taguchi's technique can be used for Design of Experiments
5. Conduct comparative studies on types of materials that can be used for manufacturing of camshafts and make a selection.
6. Validate the optimised design and analyze the results

3.3 DIFFERENT OPTIONS CONSIDERED FOR IMPROVEMENT

The target is to minimize Stress Concentration Factor for the given requirement within the specified constraints. So following approach has been considered to find an optimal solution;

1. Change in design – related to size (dimensions of existing geometry)
2. Change in design – related to shape (Make feasible changes in shape)
3. Explore materials with higher strength (Forged steels)
4. Consider change in manufacturing process as a last resort, if other things does not work

Going by the above considerations, following steps are proposed to be made;

3.3.1 Change Fillet Radius (External radius and Undercut radius)

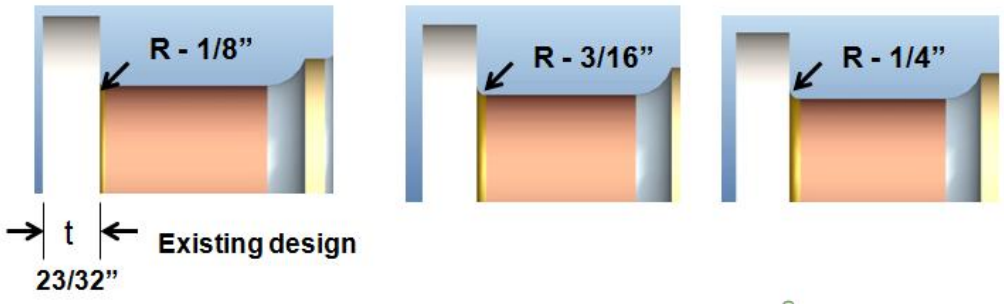

Fig:3.5 Proposed Increase in Fillet Radius

3.3.2 Increase flange thickness from existing thickness of 23/32”.

3.3.3 Optimize depth of dowel hole

As most of the failures are originating from locations closer to the dowel hole, its depth needs to be examined for bringing a change in the stress concentration factor.

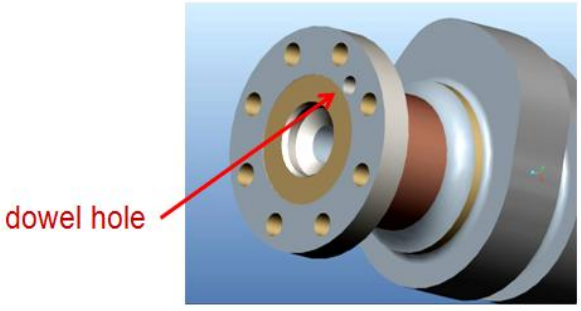

Fig: 3.6 Dowel Hole for Depth Optimization

3.3.4 PROVIDE AN UNDERCUT FILLET WITH BIGGER RADIUS

Since geometrical constraints do not permit much increase in the external fillet radius, it may prove to be beneficial to provide an undercut fillet of bigger radius, if it has the potential to reduce Stress Concentration Factor.

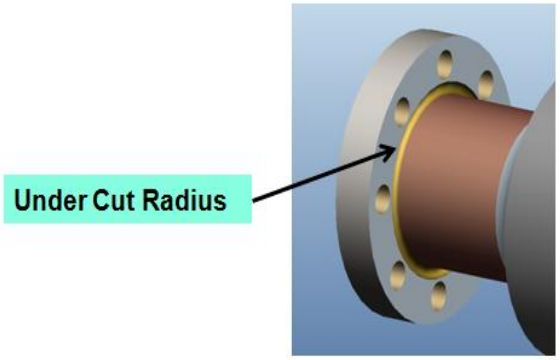

Fig: 3.7 Undercut Root Radius

3.3.5 PROVIDE VARIABLE RADIUS FILLETS

It has been observed that variable radius root can reduce SCF more that a constant radius fillets in certain loading conditions, so it will be worth exploring to try it in the present situation under torsion load.

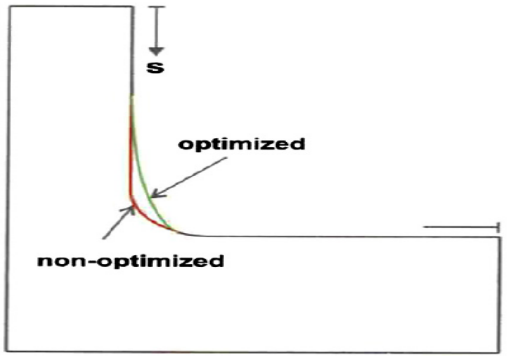

Fig: 3.8 Optimization of Variable-Root Radius[3]

3.3.6 INCREASE PCD OF COUPLING HOLES BY REDUCING THEIR SIZE AND INCREASING THE NOS.

Existing geometry has 6 coupling holes. Fillet radius can be further increased if PCD of the holes is increased. This will require reduction in their size, which can be further compensated by increase in their nos. from let say 6 to 8.

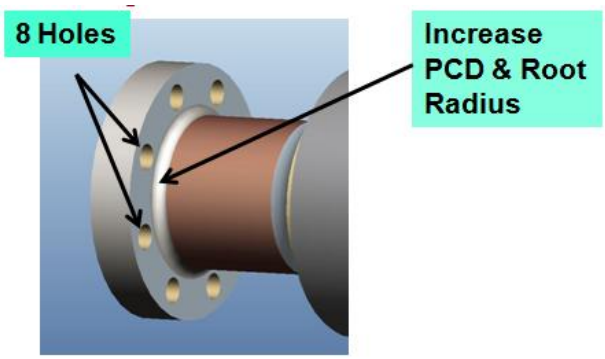

Fig: 3.9 8-Hole Configuration With More PCD

3.3.7 MATERIAL CHANGES

At present, camshafts are being manufactured out of rolled steel bars by turning and excessive removal of material. This can be replaced by forged blanks where turning operation can be considerable reduced. The main advantage anticipated is that grain flow direction in forged raw material can be controlled and it can be made parallel to the fillet radius for enhanced strength. This in turn is expected to increase the Stress Concentration Factor and finally its endurance strength. Though it involves a major change in the manufacturing process, but it will be worth exploring if it is advantageous both technically and economically.

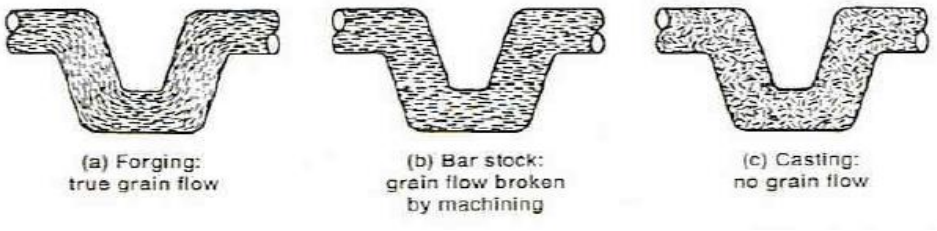

Fig. 3.10: Comparison of Grain Structure in a) Forging b) Machining c) Casting [24]

3.4 DESIGN OF EXPERIMENTS

It is proposed to try out FE analysis of the above options and then depending upon results, choose suitable combinations for optimisation.

Further it is decided to develop a forging design and conduct studies on the mechanical properties so obtained to see its effect on the vulnerable locations. It is to be validated by actual experimentation of the process.

Chapter 4

EFFECT OF VARIATIONS IN COMPONENT GEOMETRY - *FEA STUDIES*

4.1 STUDY OF COMPONENT GEOMETRY AND IN-SERVICE REQUIREMENTS

Component geometry is one of the most significant factors that determine the stress levels in various zones of the component. So a careful design process needs to adopted with due understanding of the effect of various geometrical shapes in inducing stress levels in a component. Moreover stress concentration level goes up whenever there are abrupt changes in the contour/section.

Though it is ideal to have smooth transitions from one section to other but functional requirements of a component finally dictate the geometry of the component. So a designer is to find a way so that transitions can be made smooth to the extent possible within the available envelope and other practical constraints in adopting a particular geometry. These are some of the constraints within which, a designer is supposed to find a solution;

1. Functional requirement must be met
2. Component size should not exceed the overall envelope available
3. Choice of material available
4. Manufacturability constraints
    a. Rolling, Forming, casting, forging etc.
    b. Machining constraints
    c. Heat treatment
    d. Desired level of Surface Finish
5. Assembly constraints
6. Weight constraints
7. Expected life
8. Ease of maintenance
9. Cost considerations

The current study is regarding fatigue failures in engine camshafts which work in extremely confined spaces of the engine block. The problem is further compounded by

the fact that it is a retrofit item so there is no possibility of making any change in the mating parts. Therefore, a very limited play is possible in altering the dimensions to improve upon its geometry in order to enhance the fatigue life by reducing stress concentration zones.

The investigations have revealed that the fatigue failures are occurring between the flange and the shaft where a sharp root radius has been provided. Increasing the root radius would have been the easiest option but then there are constraints related to machining.

A review of design was conducted to find out the possible forces that act on the failure zone and cause the fatigue failure.

The fatigue failure is in the nature of shear at an angle to the axis of the shaft. The prime force acting in this region is torque which is maximum in the R-9 & L-9 segments because of being the nearest to the gear drive. From design calculations of gear drive, it was revealed that the Max. Torque acting on the shaft in this region is of the order of 1980 Nm ~ 2000 Nm. Therefore an FEA of the existing design was conducted with this boundary conditions and it was revealed that the maximum stress zone occurs at the root.

4.1.1 FEM ANALYSIS

The material being a ductile material at the flange root, primarily loaded with torque, therefore a shape distortion stress will be acting on it. In such a situation Von Mises Stress calculation is the most appropriate method to analyse the components for failure.

Though there will be various dynamic stresses on the camshaft during operation of the engine but most prominent stress will be caused by the torque transmission. By design calculations, it has been computed as

$$\text{Max Torque } T_{max} = 1996 \text{ Nm } (2000 \text{ Nm})$$

For conducting FEA, the torque is simplified to an equivalent force acting on each of the six coupling holes.

The value of the force is calculated as

$$F_c = T_{max} / n X R$$

where n being number of coupling holes and

R being the pitch circle radius of coupling holes

$$F_c = 2000/ (6 X 90.5 X 10^{-3})$$

$$= 7.37 X 10^{3} N$$

Force F_c is applied tangentially at the PCD at all the six coupling holes on one flange and the surface of the opposite flange is considered as a fixed element to examine the effect of torque.

Weight of the finished component is about 22 Kg ~ 215 N

This force element on a rigidly supported member from both ends being considerably small compared to the forces acting because of torque has been ignored so as to make the model simple for study.

Solid models of SUCS has been prepared using the Creo Elements/Pro V.5.0 software. The Solid model has further been used for FEA meshing. Meshing has been done using Hypermesh v09 Software. FEM modelling has been done using Tetrahedral elements.. RADIOSS solver has been used for Linear Static Analysis.

Both 2D & 3D elemental stresses have been considered.

Size of the element : 2 mm

Number of elements : 521843 ~ 5.20 X 10^5

Number of nodes : 114208 ~ 1.14 X 10^5

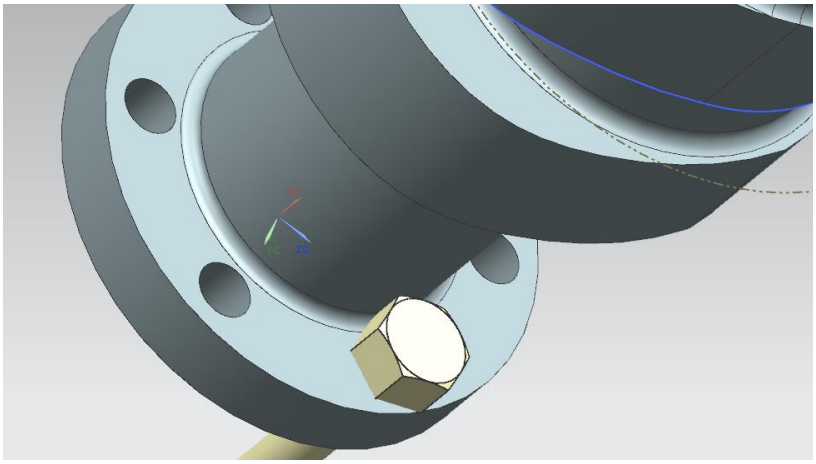

Fig 4.1: Arrangement showing the coupling and coupling screw resisting the torque

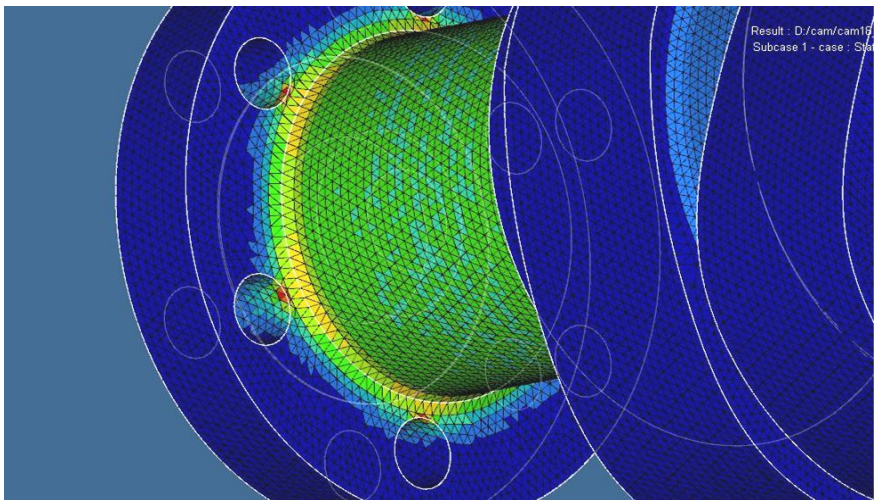

Fig 4.2: Meshing done using HyperMesh Hypermesh v09 Software (Element size 2mm)

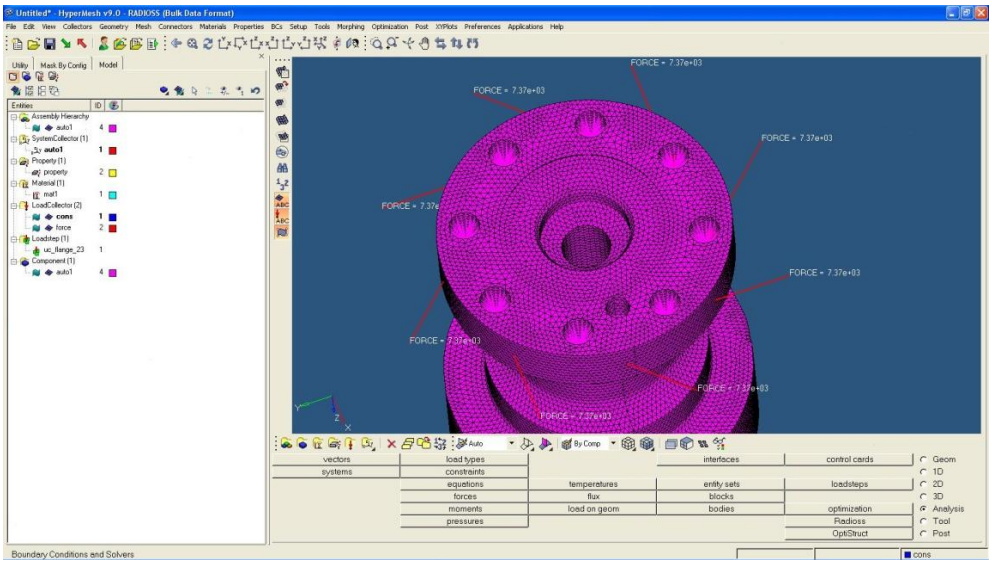

Fig 4.3: Model with tangential force component in meshed condition

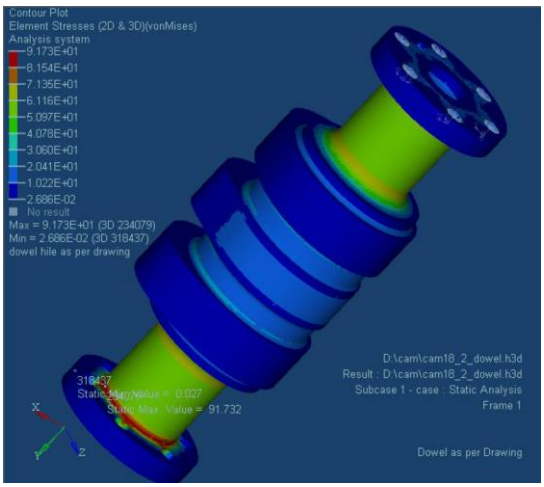

Fig 4.4: FEA of the existing model showing Max Stress of 91.7 MPa (Von Mises)

From this modelling, Value of Max. Stress obtained has been **91.7 MPa** and it is considered as base value for seeing effet of variuos other parameters to be experimented with.

4.2 STUDY OF EXISTING MANUFACTURING PROCESS

Different options to be considered for bringing changes in component geometry can only be applied if the entire process of manufacturing and assembly is studied in detail. So, manufacturing process was studied with the objective of identifying any manufacturing constraints and the assembly procedure.

4.2.1 EXISTING MANUFACTURING PROCESS

i. Raw material for the component is procured from steel manufacturers to Railway Specification No. D81602 equivalent to AISI E1070 (high carbon steel) in the form of normalised & tempered hot rolled steel bars of Ø 160mm.

ii. The bars are cut into blanks on a band saw machine to length of 360 mm.

iii. The two ends of the blank are faced and centres are drilled on a double end facing and centring machine.

iv. The job is turned on a CNC turning centre to generate the flanges at two ends and cylindrical blanks for milling of cam profiles.

v. In order to identify the component, a manufacturer's product serial number is punched on one end of a flange.

vi. A dowel hole of Ø 9.5mm X 17.72 mm deep is drilled on the flange on a radial drilling machine. In reference to the first dowel, another dowel hole of same size is drilled in the opposite flange.

vii. A gun drilling operation is carried out on the job to drill a through hole of dia Ø 19.05 mm which provides a passage for the lubrication oil during opration.

viii. Thereafter the job is loaded on a CNC Turn-Mill Centre for cam profile milling, where it is held on a 4 jaw chuck and the job is referenced from the dowel hole. All three cam lobes are milled in one setting one by one by edge milling cutters.

ix. Deburring operation is carried out manually for removing burrs from machined edges.

x. Then induction hardening of lobes is done on CNC Induction Hardening machine in order to achieve a hardness of 58-62 Rc after tempering to achieve a case depth of 3 -6 mm.

xi. A cylindrical grinding operation is carried out to maintain the size within specified tolerances on the flange diameters.

xii. Co-bores are machined on the two ends on a CNC turning machine.

xiii. Thereafter coupling holes are drilled on radial drilling machines using jigs.

xiv. Cam profiles are ground on CNC Cam Profile grinding machine to achieve surface finish below 5 μm.

xv. A spot facing operation is done on the coupling holes on the flange

xvi. The final component is finished by de-burring and inspected.

4.3 STUDY OF THE EXISTING ASSEMBLY PROCESS

It is important to understand the existing assembly process of the camshaft segments on the engine block so that constraints, if any, can be visualised before any alterations are made in the component geometry.

4.3.1 EXISTING ASSEMBLY PROCESS

The camshaft segments form part of the two assembled camshafts for Left Hand and Right Hand bank of the 16-Cylinder V-Engine. Each camshaft assembly has 8 camshaft segments separated by 7 spacers and two end pieces which are supported in 9 camshaft bores provided in the engine block. Coated brass bushes are provided in all camshaft bores which are lubricated by pressurized lube oil coming out of oil holes in the bearing area of spacers.

The assembly sequence is as follows;

i. The seven spacers and two end pieces each for the LH & RH side are press fitted with dowel pins of Ø 9.5mm X 25.4 mm. The spacers have dowels on both sides whereas end pieces have dowel on one end only.

ii. The identical camshaft segments (8 nos. each for RH & LH) are assembled to the spacers in pre-determined sequence by locating dowels and Allen screws of ½" nominal dia X 1-1/2" long.

iii. After torquing of screws, the entire assembly is put on two V-blocks on a surface table and its run-out is checked at all other bearing surfaces to ensure straightness and concentricity of the assembled camshaft.
iv. After validation of assembly, it is dismantled and the assembly process is started on the engine block.
v. On one end of the camshaft on engine block is fitted an outboard housing with thrust bearings. This act as a support for starting of the camshaft assembly process.
vi. All the numbered spacers are placed in their respective camshaft bore bearings.
vii. Camshaft segments are inserted one-by-one from the front openings and aligned with the spacer dowels and assembled with the help of Allen Screws.
viii. Once the entire shaft is assembled, the screws are torqued to a pre-defined torque value.
ix. The other end of the camshaft is held by an over speed trip assembly fitted on the engine block.

Main Observations during assembly:

i. The opening in the engine block is just enough for inserting the camshaft segments. Any change in the length of the camshaft segment will require a major modification in the engine block, thus considered as a constraint.
ii. The Allen screws are of 1-1/2" length. There is a very limited scope for increase of the flange width else the screw cannot be inserted.
iii. The head diameter of the screw is ¾". To accommodate the head in its location, the root radius of the flange cannot be increased at all from the existing level of 1/16" else the head will not seat properly.

4.4 DIFFERENT OPTIONS FOR CHANGES IN GEOMETRY

With these initial inputs and with an objective of reducing the max induced stress, different changes in the geometry of the component were envisaged. These are;

1. Increase in flange width
2. Increase root radius of the flange
3. Increase PCD of coupling holes
4. Consider introducing variable radius
5. Examine depth of dowel hole
6. Provide undercut radius

Since the component under consideration is a complex geometry, it has already been observed in literature review that standard or empirical relations are not available for computation of maximum induced stress. So Finite Element Analysis method was adopted by providing suitable boundary conditions and record the variations observed during FEA with respect to each parameter considered above. In the ensuing report, feasibility of adoption of each of the above options and their effect on the maximum stress level as obtained in FEA is elaborated.

4.4.1 EFFECT OF UNDERCUT RADIUS IN THE FLANGE ON MAX. STRESS

In the existing design, the root radius is 1/16" (1.6 mm) and is one of the causes of stress concentration. Further there is no scope for increasing this radius due to fastening constraints. So in order to increase the curvature at the root, it was considered as an option to provide an undercut with higher radius at the root. Further it is possible to provide this radius both in the flange as well as in the shaft. So both options were tried one by one. Initially a radius was tried in the flange as shown in the figure.

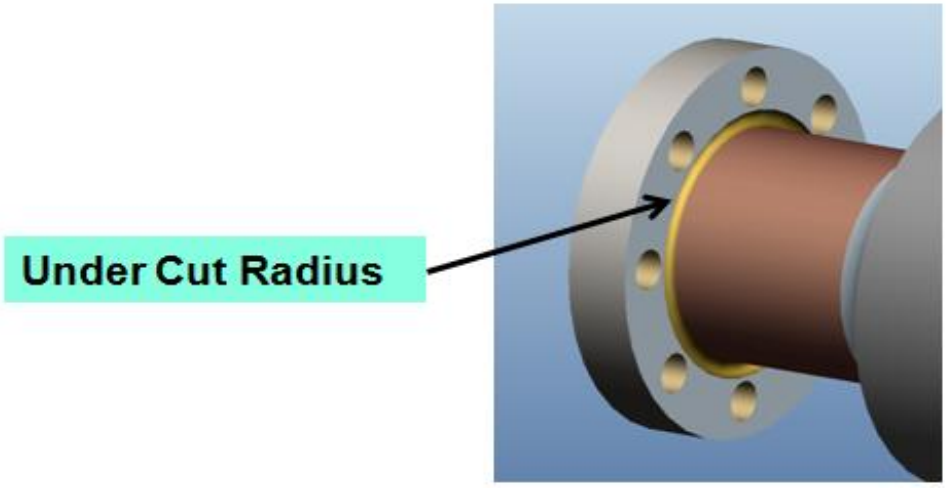

Fig 4.5: 3-D Model depicting undercut groove in the flange at the location of stress concentration zone

4.4.1.1 Constraints in the Configuration

As we provide a undercut in the flange, the cross-section will become weak. So when radius is to be provided, corresponding increase is required in the flange thickness. There is a limit up to which flange thickness can be increased due to assembly constraints explained earlier.

Another constraint in increasing the radius is the coupling holes. The radius of the undercut should not intersect the coupling holes.

Within these constraints, three different radii were tried to see if any improvement is achieved and at the same time what is pattern of this increase with respect the increase in radius.

Accordingly three 3-D models were developed with following radii in the flange groove:

Table 4.1: Three proposed models with variations in undercut radius in flange

Model	**Radius of Undercut in Flange (mm)**	**Flange Thickness (mm)**
M-1	2.16	20.42
M-2	2.54	20.80
M-3	2.92	21.18

4.4.1.2 FEM Analysis

The material being a ductile material at the flange root, primarily loaded with torque, therefore a shape distortion stress will be acting on it. In such a situation Von Mises Stress calculation is the most appropriate method to analyse the components for failure.

Though there will be various dynamic stresses on the camshaft during operation of the engine but most prominent stress will be caused by the torque transmission. By design calculations, it has been computed as

Max Torque T_{max} = 1996 Nm (2000 Nm)

For conducting FEA, the torque is simplified to an equivalent force acting on each of the six coupling holes.

The value of the force is calculated as

$$F_c = T_{max} / n \, X \, R$$

where n being number of coupling holes and

R being the pitch circle radius of coupling holes

$$F_c = 2000/ (6 X 90.5 X 10^{-3})$$

$$= 7.37 X 10^{3} N$$

Force F_c is applied tangentially at the PCD at all the six coupling holes on one flange and the surface of the opposite flange is considered as a fixed element to examine the effect of torque.

Weight of the finished component is about 22.3 Kg ~ 218.54 N

This force element on a rigidly supported member from both ends being considerably small compared to the forces acting because of torque has been ignored so as to make the model simple for study.

Solid models of SUCS has been prepared using the Creo Elements/Pro V.5.0 software. The Solid model has further been used for FEA meshing. Meshing has been done using Hypermesh v09 Software. FEM modelling has been done using Tetrahedral elements.. RADIOSS solver has been used for Linear Static Analysis.

Both 2D & 3D elemental stresses have been considered.

Size of the element : 2 mm

Number of elements : 531735 ~ 5.31 X 10^5

Number of nodes : 114486 ~ 1.14 X 10^5

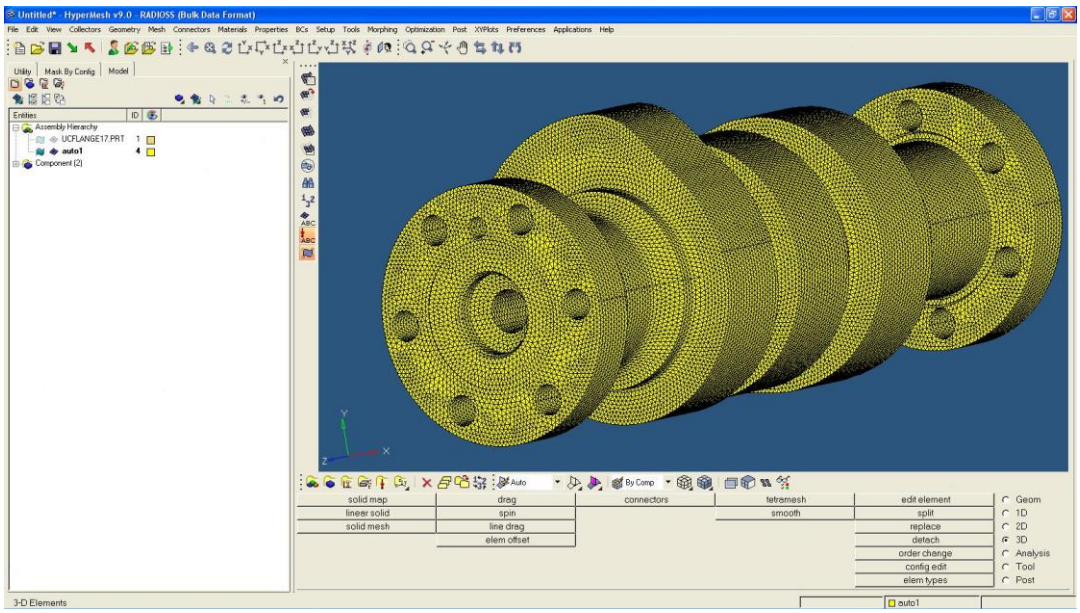

Fig.4.6 : Meshing done on Hypermesh v09 Software using Tetrahedral elements of 2mm size with undercut in flange

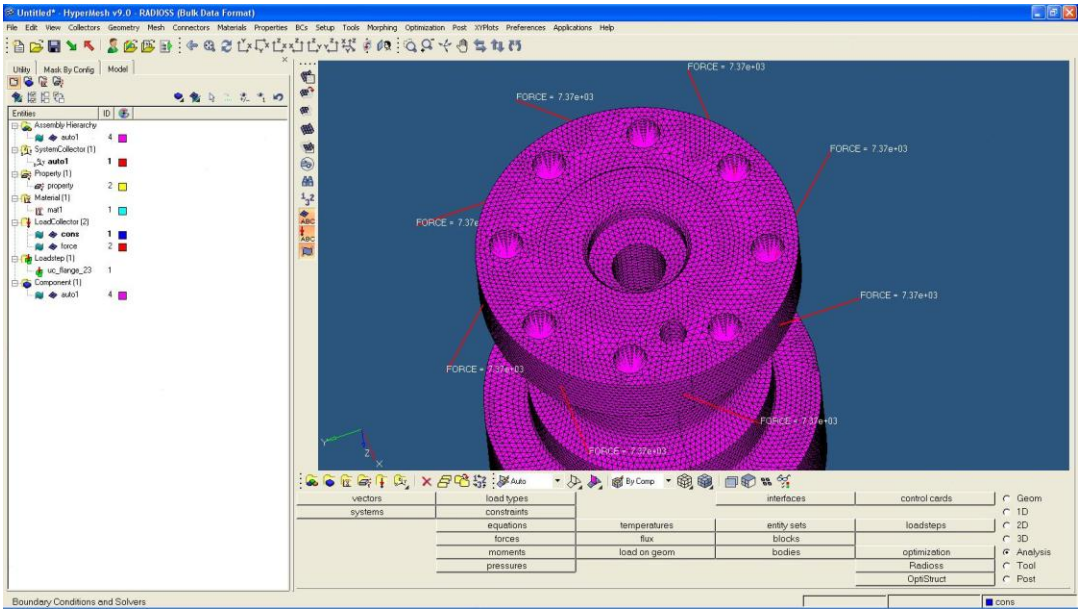

Fig 4.7 : Conversion of torque into equivalent force elements applied at PCD before FEA (with undercut in flange)

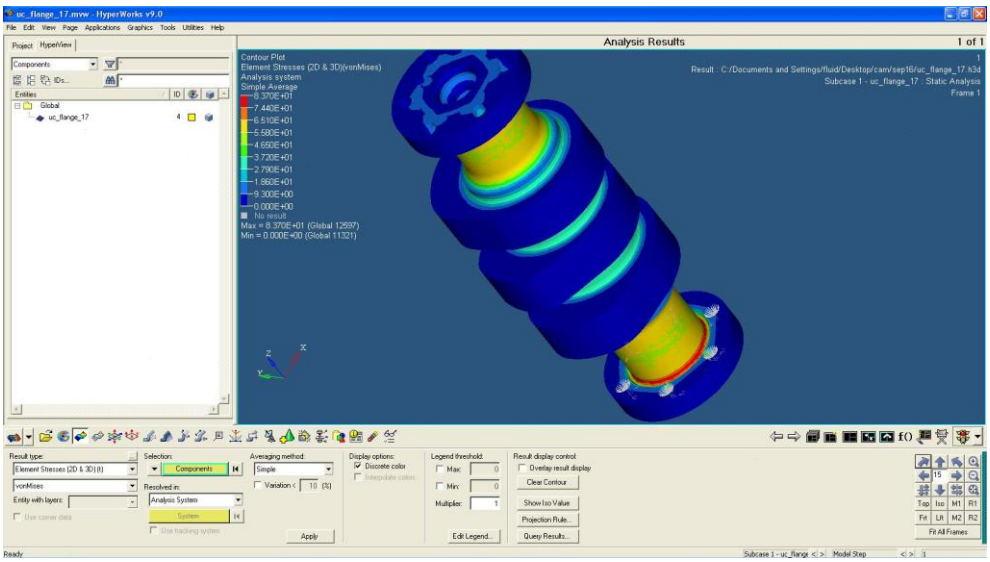

Fig 4.8 : FEA of the meshed model with undercut radius 2.16 mm on RADIOSS solver

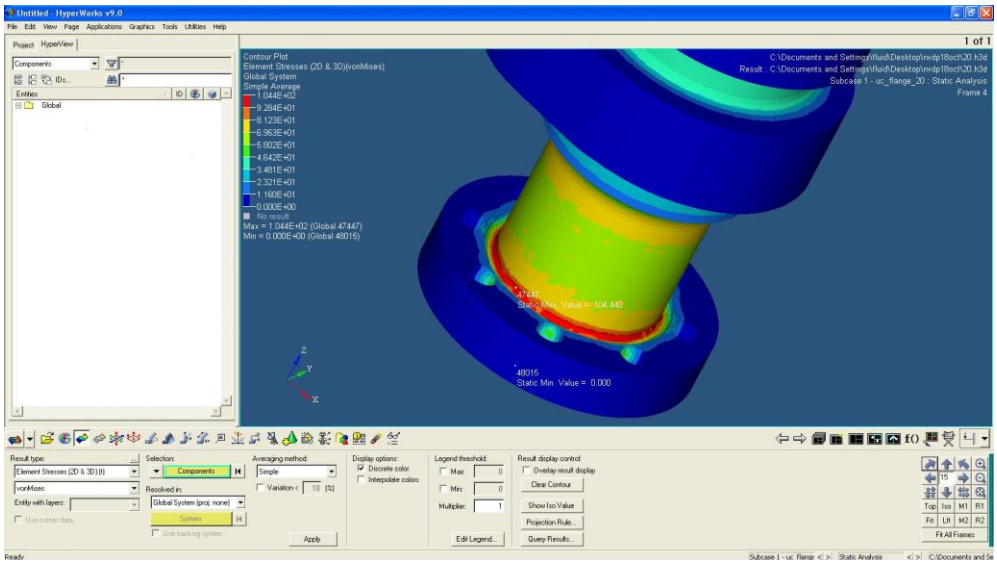

Fig 4.9 : FEA of the meshed model with undercut radius 2.54 mm on RADIOSS solver

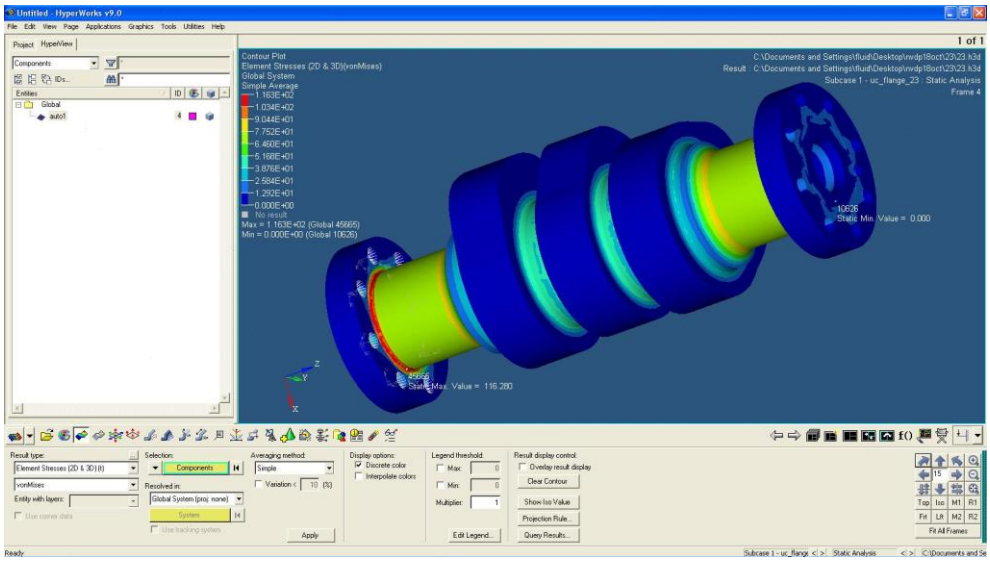

Fig 4.10: FEA of the meshed model with undercut radius 2.92 mm on RADIOSS solver

FEA results from this experiment are tabulated below;

Table 4.2 : Results obtained from FEA by introducing undercut radius in the flange

Sr	Radius of Undercut in Flange (mm)	Flange Thickness (mm)	Max Stress Von Mises (MPa)
1	2.16	20.42	83.7
2	2.54	20.80	104.4
3	2.92	21.18	116.0

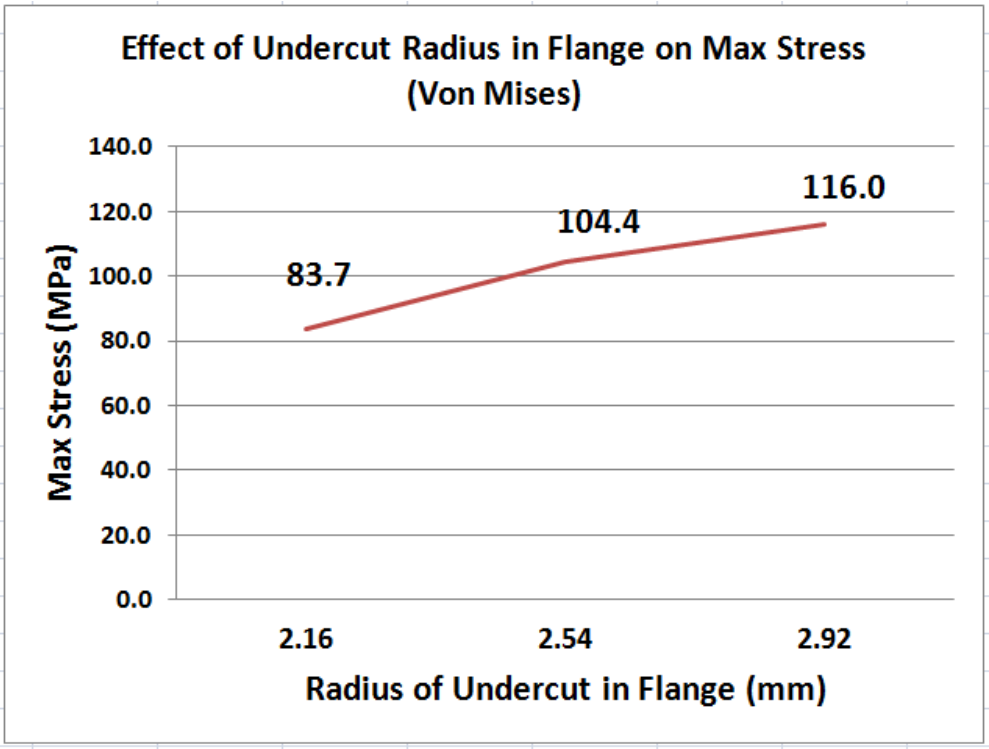

Fig 4.11: Plot showing variation in Max Stress (Von Mises) w.r.t. undercut radius in flange

4.4.1.3 Results

It is observed that the increase in undercut radius is in fact increasing the stress level and it is happening at the root end. This may be attributed to the reason that providing an undercut near the dowel is leading to a weaker section and causing stress concentration on the outer edge of the radius close to the dowel hole.

4.4.2 EFFECT OF UNDERCUT RADIUS IN SHAFT ON MAX STRESS

After getting the results for the undercut radius in the flange and analysing the reasons for increase in stress level, an undercut was tried in the shaft near the root, blending its one end with the flange for smooth transition. Since this groove will be away from the dowel hole and other stress concentrating features, it was expected to improve the geometry and reduce the overall stress level, So an undercut groove was provided and the flange as shown in Fig. 4.12.

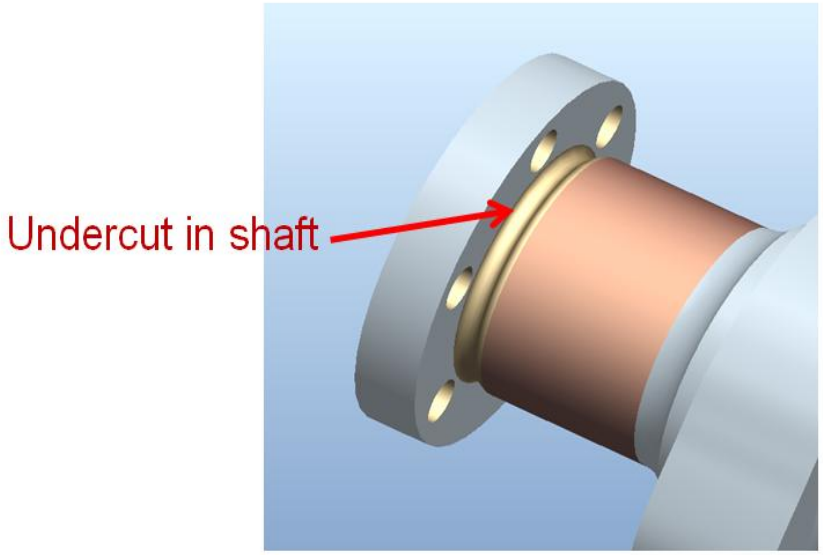

Fig 4.12 : 3-D Model depicting undercut radius in the shaft at the location of stress concentration zone

4.4.2.1 Constraints in the Configuration

As we provide an undercut in the grrove, the cross-section of the shaft will become weak. So when radius is to be provided, corresponding increase is required in the shaft diameter. There is a limit up to which flange thickness can be increased due to assembly constraints explained earlier.

In order to eliminate the sharp edge at the end of radius, it was blended with an equal radius in the opposite direction towards the shaft end as depicted in the picture.

Within these constraints, three different radii were tried to see if any improvement is achieved and at the same time what is pattern of this increase with respect the increase in radius. Accordingly three 3-D models were developed with following radii in the flange groove:

Table 4.3: Three proposed models with variations in undercut radius in shaft

Model	Radius of Undercut in Shaft (mm)	Compensated Diameter of Shaft (mm)
M-1	1.52	70.92
M-2	2.29	72.44
M-3	3.05	73.96

4.4.2.2 FEM Analysis

The material being a ductile material at the flange root, primarily loaded with torque, therefore a shape distortion stress will be acting on it. In such a situation Von Mises Stress calculation is the most appropriate method to analyse the components for failure.

Though there will be various dynamic stresses on the camshaft during operation of the engine but most prominent stress will be caused by the torque transmission. By design calculations, it has been computed as

Max Torque T_{max} = 1996 Nm (2000 Nm)

For conducting FEA, the torque is simplified to an equivalent force acting on each of the six coupling holes.

The value of the force is calculated as

$$F_c = T_{max} / n \, X \, R$$

where n being number of coupling holes and

R being the pitch circle radius of coupling holes

$$F_c = 2000/ (6 \, X \, 90.5 \, X \, 10^{-3})$$

$$= 7.37 \, X \, 10^{3} \, N$$

Force F_c is applied tangentially at the PCD at all the six coupling holes on one flange and the surface of the opposite flange is considered as a fixed element to examine the effect of torque.

Weight of the finished component is about 22.6 Kg ~ 221 N

This force element on a rigidly supported member from both ends being considerably small compared to the forces acting because of torque has been ignored so as to make the model simple for study.

Solid models of SUCS has been prepared using the Creo Elements/Pro V.5.0 software. The Solid model has further been used for FEA meshing. Meshing has been done using Hypermesh v09 Software. FEM modelling has been done using Tetrahedral elements.. RADIOSS solver has been used for Linear Static Analysis.

Both 2D & 3D elemental stresses have been considered.

Size of the element : 2 mm

Number of elements : 5379043 ~ 5.37 X 10^5

Number of nodes : 116423 ~ 1.16 X 10^5

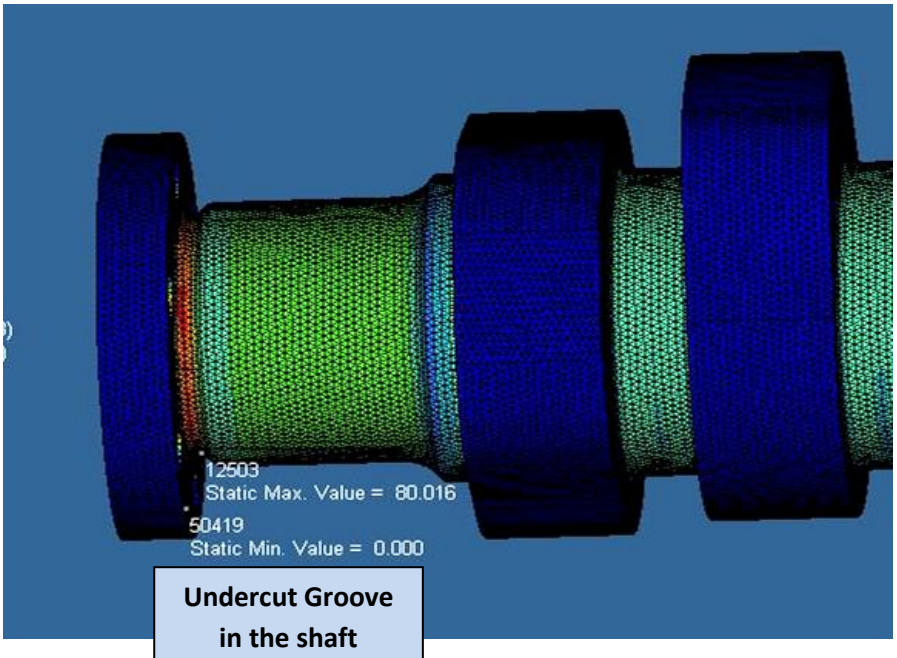

Fig 4.13: Meshing done on Hypermesh v09 Software using Tetrahedral elements of 2mm size (With undercut grove in shaft)

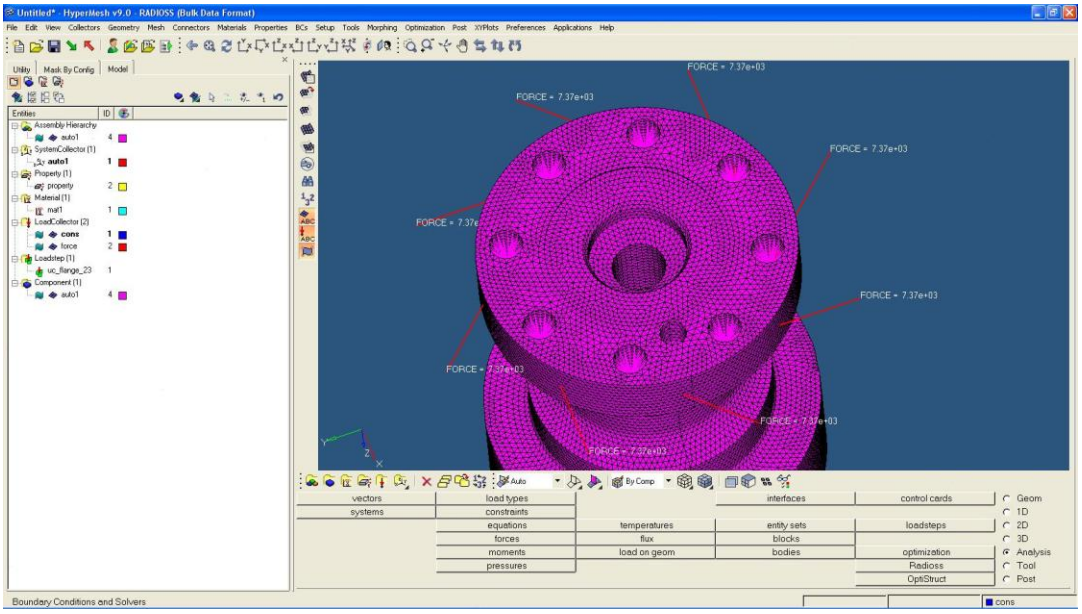

Fig 4.14 : Conversion of torque into equivalent force elements applied at PCD before FEA (With undercut grove in shaft)

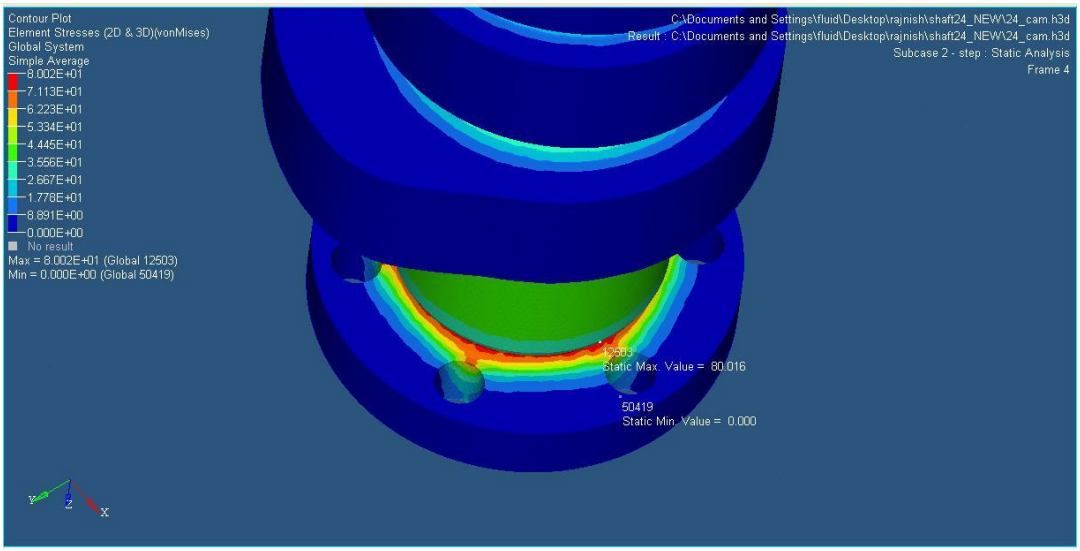

Fig 4.15 : FEA of the meshed model with undercut radius 2.92 mm on RADIOSS solver

FEA results from this experiment are;

Table 4.4: Results obtained from FEA by introducing undercut radius in the shaft

Model	Radius of Undercut in Shaft (mm)	Compensated Diameter of Shaft (mm)	Max Stress Von Mises (MPa)
M-1	1.52	70.92	86.5
M-2	2.29	72.44	83.6
M-3	3.05	73.96	80.0

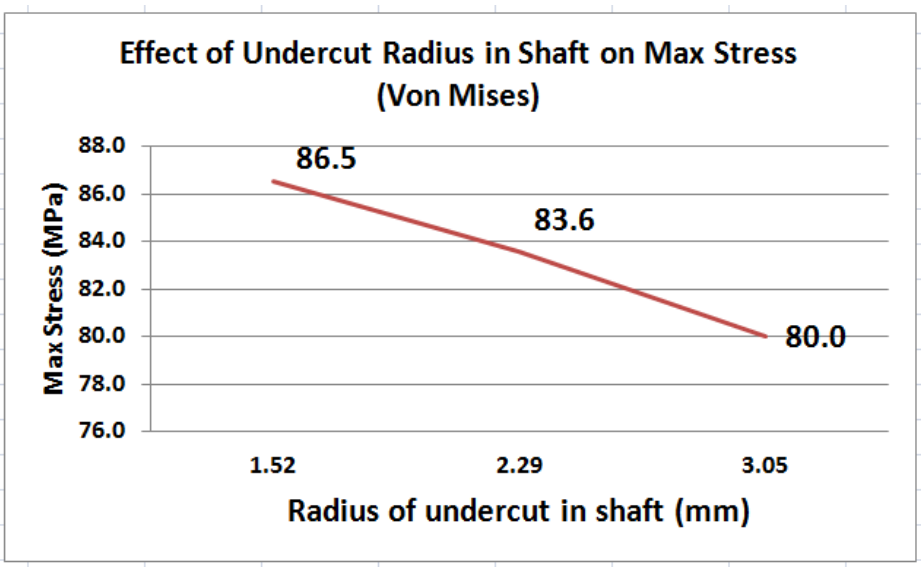

Fig 4.16: Plot showing variation in Max Stress (Von Mises) w.r.t. undercut radius in shaft

4.4.2.3 Results:

1. It is observed that the increase in undercut radius on the shaft side is resulting in reducing the maximum stress level.
2. When compared with base model, it is seen that stress level comes down to 80.0 MPa on introduction of undercut from an initial stress level of 91.7 mm.

4.4.3 EFFECT OF INCREASING FLANGE THICKNESS OF SHAFT ON MAX STRESS

Due to a co-bore in the camshaft design, the cross-section near the flange root may become weak. So, it was considered one of the options to increase the flange width, so as to strengthen the cross section and see its effect. Increasing the flange thickness is expected to provide more material over the fixed depth co-bore thus may lead to lower level of stresses due lesser abruption in the component geometry.

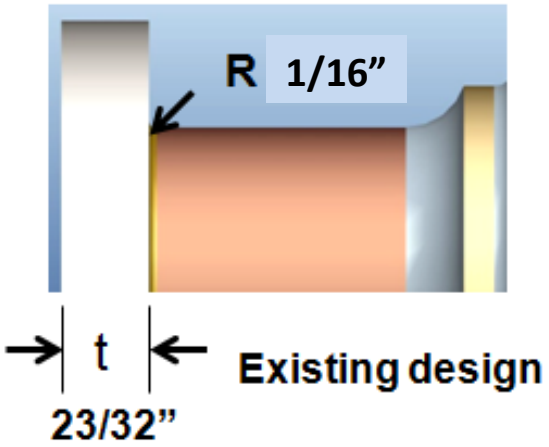

Fig 4.17 : 3-D Model depicting flange width near stress concentration zone

4.4.3.1 Constraints in the Configuration:

There is a constraint imposed by assembly that if we increase the flange width, the length of the fastener will have to be increased to that extent and there is a limitation up to which a longer fastener can be accommodated.

The overall width of the component is to be maintained with existing overall dimension therefore any increase in flange width will have to be compensated with corresponding reduction in the length of other members.

The location of cam lobes is fixed as these are mating with cam rollers provided over Lifter X-head and Lifter Push Rod therefore no change can be incorporated in this area.

The compensation can be provided only in the cylindrical members just next to the flanges.

Within these constraints, three different flange thicknesses were tried to see if any improvement is achieved and at the same time what is pattern of this increase with respect the increase in radius.

Based on the available envelope, it was seen that the flange width can be increased from 18.26 mm to a maximum of 26.99 mm with corresponding reduction in the length of cylindrical features next to the flange. Accordingly three models were prepared using Creo Elements/Pro 5.0 3-D modelling software by varying the flange thickness.

Table 4.5: Three proposed models with variations in flange thickness

Model	Flange Thickness (mm)	Compensated Length of Shaft (mm)
M-1	18.26	65.88
M-2	22.23	61.91
M-3	26.99	57.15

4.4.3.2 FEM Analysis

The material being a ductile material at the flange root, primarily loaded with torque, therefore a shape distortion stress will be acting on it. In such a situation Von Mises Stress calculation is the most appropriate method to analyse the components for failure.

Though there will be various dynamic stresses on the camshaft during operation of the engine but most prominent stress will be caused by the torque transmission. By design calculations, it has been computed as

Max Torque T_{max} = 1996 Nm (2000 Nm)

For conducting FEA, the torque is simplified to an equivalent force acting on each of the six coupling holes.

The value of the force is calculated as

$$F_c = T_{max} / n \, X \, R$$

where n being number of coupling holes and

R being the pitch circle radius of coupling holes

$$F_c = 2000/ (6 \text{ X } 90.5 \text{ X } 10^{-3})$$

$$= 7.37 \text{ X } 10^{3} \text{ N}$$

Force F_c is applied tangentially at the PCD at all the six coupling holes on one flange and the surface of the opposite flange is considered as a fixed element to examine the effect of torque.

Weight of the finished component is about 23.1 Kg ~ 225 N

This force element on a rigidly supported member from both ends being considerably small compared to the forces acting because of torque has been ignored so as to make the model simple for study.

Solid models of SUCS has been prepared using the Creo Elements/Pro V.5.0 software. The Solid model has further been used for FEA meshing. Meshing has been done using Hypermesh v09 Software. FEM modelling has been done using Tetrahedral elements.. RADIOSS solver has been used for Linear Static Analysis.

Both 2D & 3D elemental stresses have been considered.

Size of the element : 2 mm

Number of elements : 542789 ~ 5.42 X 10^5

Number of nodes : 117348 ~ 1.17 X 10^5

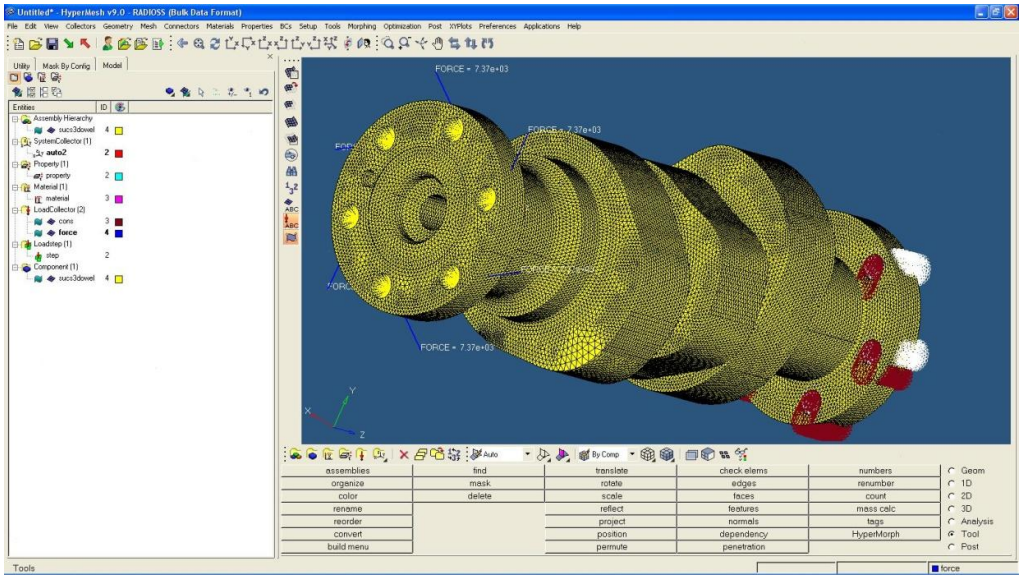

Fig 4.18 : Meshing done on Hypermesh v09 Software using Tetrahedral elements of 2mm size (with increased flange thickness)

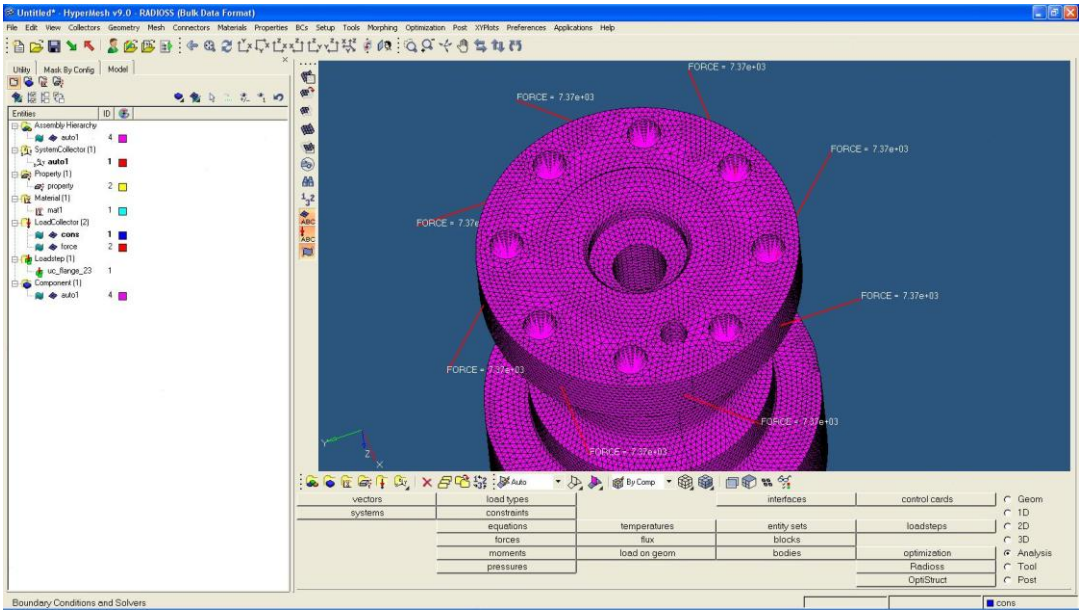

Fig 4.19: Conversion of torque into equivalent force elements applied at PCD before FEA (with increased flange thickness)

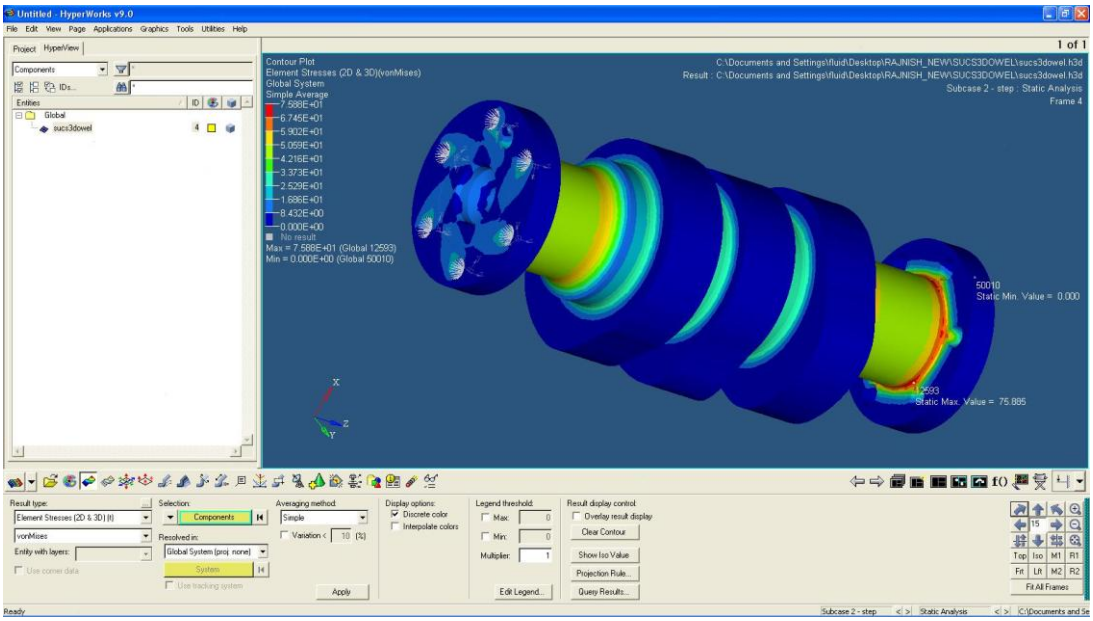

Fig 4.20: FEA of the meshed model with increased flange thickness of 26.99 mm on RADIOSS solver

FEA results from this experiment are;

Table 4.6: Results obtained from FEA by increasing flange thickness

Model	Flange Thickness (mm)	Compensated Length of Shaft (mm)	Max Stress Von Mises (MPa)
M-1	18.26	65.88	82.1
M-2	22.23	61.91	78.54
M-3	26.99	57.15	75.88

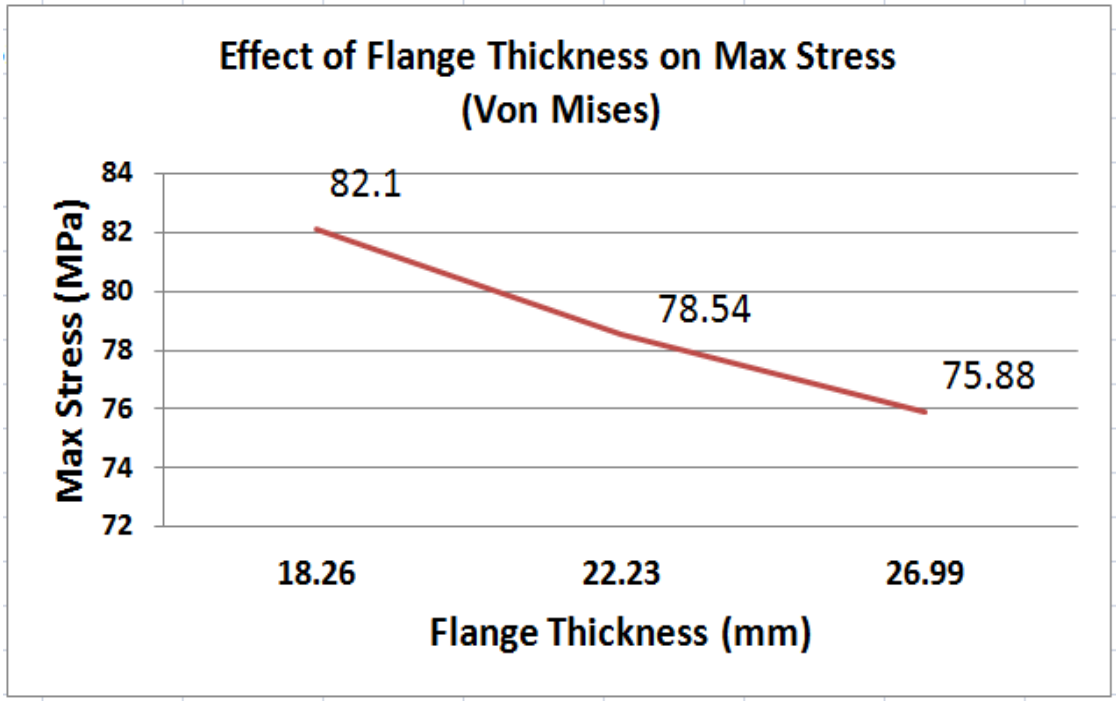

Fig 4.21: Plot showing variation in Max Stress (Von Mises) w.r.t. increase in flange thickness

4.4.3.3 Results:

1. It is observed that the increase in flange thickness with corresponding reduction in length of cylindrical feature of the camshaft is resulting in reducing the maximum stress level.
2. When compared with base model, it is seen that stress level is continuously coming down from a value of 82.1 MPa for the base model to a value of 75.88 MPa.

4.4.4 EFFECT OF REDUCTION IN DEPTH OF DOWEL HOLE ON MAX STRESS

It is observed that dowel holes provided for relative alignment of matching components also lead to sudden notching in the cross-section and may also lead to a stress concentration zone by fatigue theory. So in order to assess its effect on the component geometry, variations in its locations and size were considered. The dowel hole is centrally located between the coupling holes in such a manner that maximum metal condition can be achieved. By this logic it should be close to centre axis, but then there are chances of increasing the error due to tolerance provided for machining.

So the optimum location for the dowel is to locate it as far as possible from the component axis and at the same time it should be at a radial distance which is less than the PCD of the coupling holes. This will ensure that the location error is minimised due to machining tolerance of the dowel hole.

The other possible variation is in its length. Extensive survey of literature has revealed that it is only the diameter and tolerances for fits have been studied in detail and industry standards are available. But the length of the dowel pins is as per user requirement and no literature and study is available on the subject.

But components like this camshaft which have a through hole/bore are further constrained by ID of the bore as maximum metal conditions become difficult arrive at. So this aspect also needs to be seen in this case.

So effect of length of dowel pin on the fatigue life of a component in this situation becomes a topic of study.

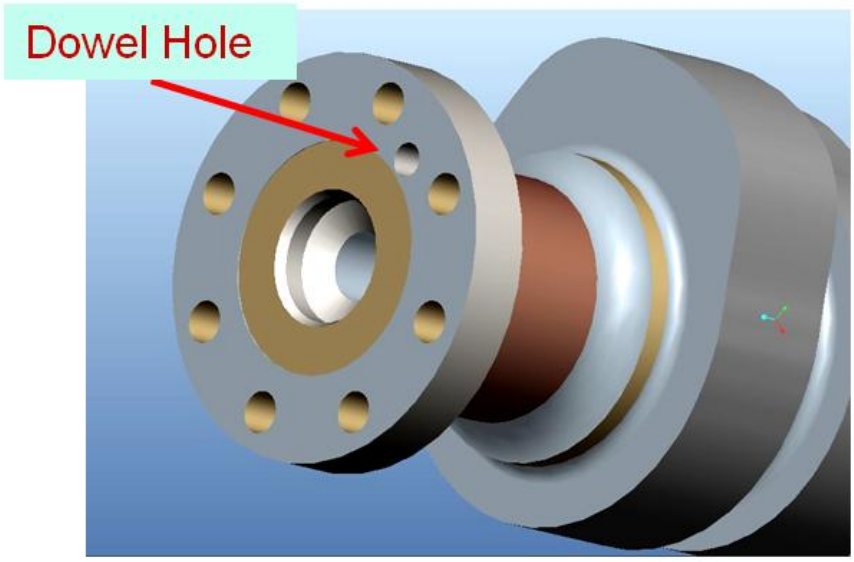

Fig 4.22: 3-D Model depicting dowel hole depth near stress concentration zone

4.4.4.1 Constraints in the Configuration:

As mentioned above, the constraints for location of dowel in our current study are;

1. To locate the dowel hole as far as possible from the centre axis so that error introduced due to machining tolerances is minimised.
2. Locate it in the middle of any two coupling holes.
3. Due to through hole and also a co-bore in the component geometry, the maximum metal conditions are required to be observed.
4. The diameter of the pin is chosen based on standard values for size of the coupling flange.

Within these constraints, it is observed that location and diameter of the pin has been chosen properly in the existing design.

So the next option is to see if the depth of the dowel hole has any significance. It can vary from a size equal to the diameter of the pin to as long as a through hole in the flange of the camshaft segment. It does not require any other modification in the geometry except for change in the length of dowel pin.

Based on above studies, it was decided that three models be developed by varying the dowel hole depth from 7.62 mm to 17.78 mm (through hole). Accrdingly length of dowel pin was varied. Accordingly three models were prepared using Creo Elements/Pro 5.0 3-D modelling software by varying the dowel hole depth as follows.

Table 4.7: Three proposed models with variations in dowel hole depth

Model	Depth of dowel pin hole in flange (mm)	Length of dowel pin(mm)
M-1	17.78	25.40
M-2	12.70	20.32 ~ 20
M-3	7.62	15.24 ~ 15

4.4.4.2 FEM Analysis

The material being a ductile material at the flange root, primarily loaded with torque, therefore a shape distortion stress will be acting on it. In such a situation Von Mises Stress calculation is the most appropriate method to analyse the components for failure.

Though there will be various dynamic stresses on the camshaft during operation of the engine but most prominent stress will be caused by the torque transmission. By design calculations, it has been computed as

Max Torque T_{max} = 1996 Nm (2000 Nm)

For conducting FEA, the torque is simplified to an equivalent force acting on each of the six coupling holes.

The value of the force is calculated as

$$F_c = T_{max} / n \, X \, R$$

where n being number of coupling holes and

R being the pitch circle radius of coupling holes

$$F_c = 2000/ (6 \, X \, 90.5 \, X \, 10^{-3})$$

$$= 7.37 \, X \, 10^{3} \, N$$

Force F_c is applied tangentially at the PCD at all the six coupling holes on one flange and the surface of the opposite flange is considered as a fixed element to examine the effect of torque.

Weight of the finished component is about 22 Kg ~ 215 N

This force element on a rigidly supported member from both ends being considerably small compared to the forces acting because of torque has been ignored so as to make the model simple for study.

Solid models of SUCS has been prepared using the Creo Elements/Pro V.5.0 software. The Solid model has further been used for FEA meshing. Meshing has been done using Hypermesh v09 Software. FEM modelling has been done using Tetrahedral elements.. RADIOSS solver has been used for Linear Static Analysis.

Both 2D & 3D elemental stresses have been considered.

Size of the element : 2 mm

Number of elements : 521843 ~ 5.20 X 10^5

Number of nodes : 114208 ~ 1.14 X 10^5

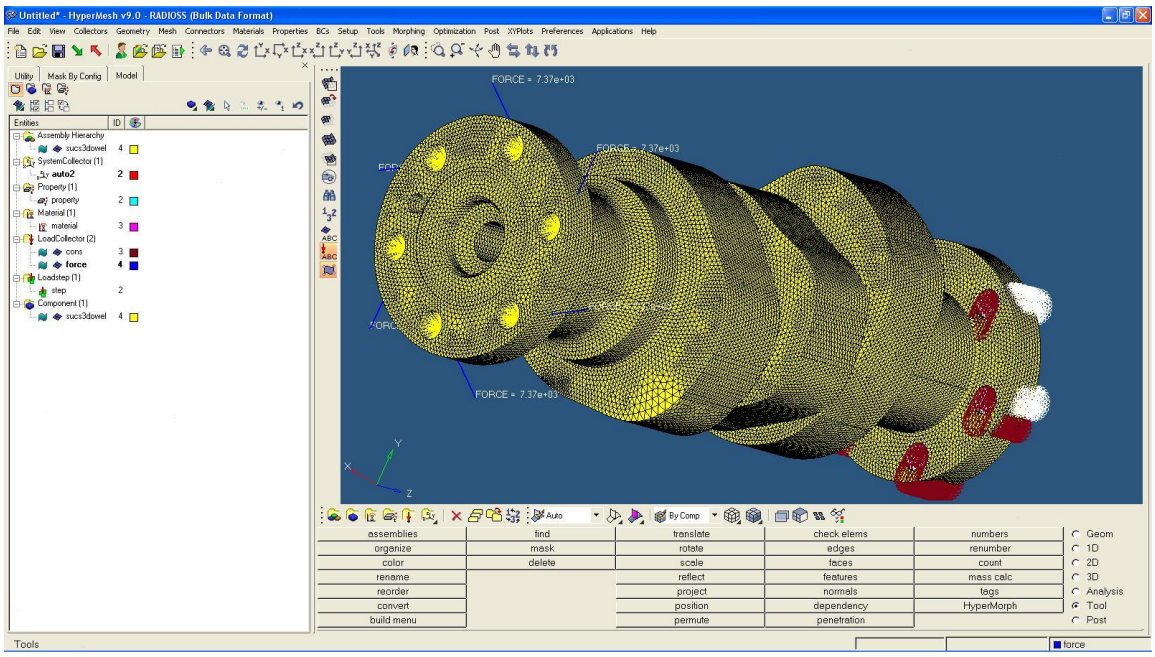

Fig 4.23 : Meshing done on Hypermesh v09 Software using Tetrahedral elements of 2mm size (with reduced dowel hole depth)

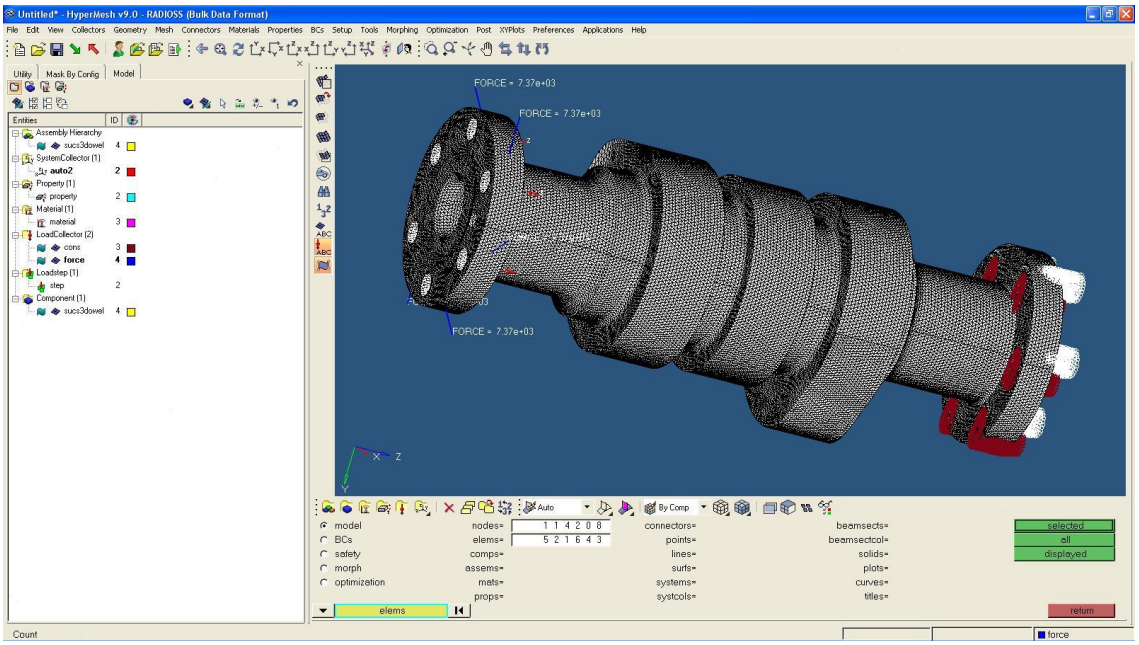

Fig 4.24 : Conversion of torque into equivalent force elements applied at PCD before FEA (with reduced dowel hole depth)

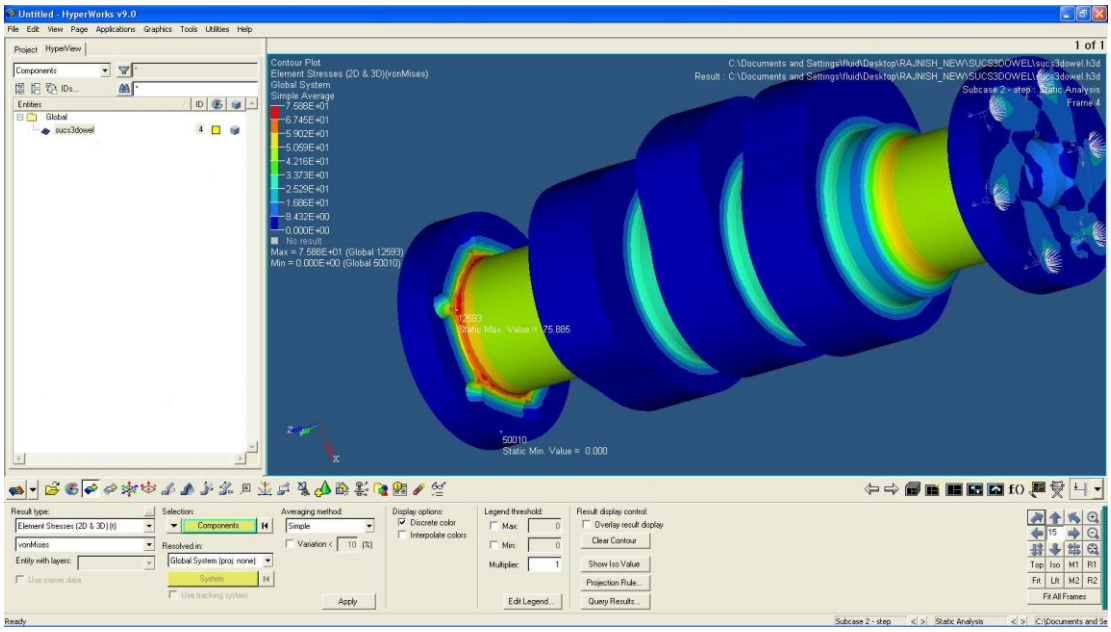

Fig 4.25 : FEA of the meshed model with dowel hole depth of 12.7 mm on RADIOSS solver

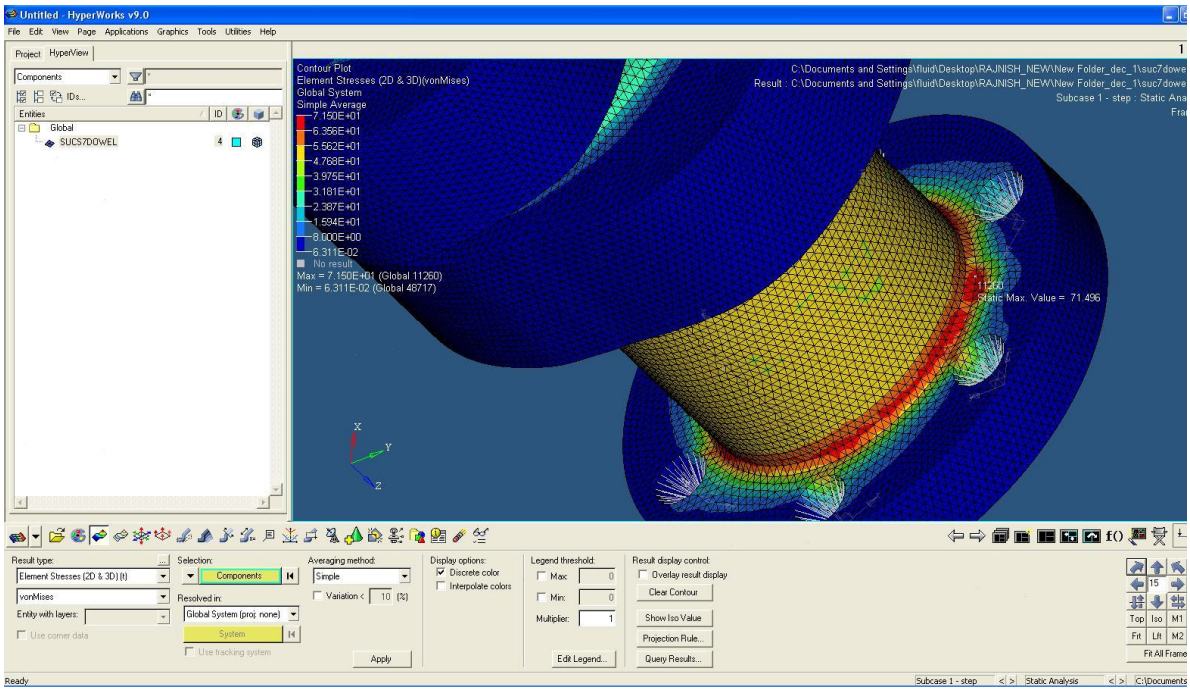

Fig 4.26 : FEA of the meshed model with dowel hole depth of 7.62 mm on RADIOSS solver

FEA results from this experiment are;

Table 4.8: Results obtained from FEA by reducing the depth of dowel hole

Model	Depth of dowel pin hole in flange (mm)	Length of dowel pin (mm)	Max Stress Von Mises (MPa)
M-1	17.78	25.40	82.2
M-2	12.70	20.32 ~ 20	75.88
M-3	7.62	15.24 ~ 15	71.5

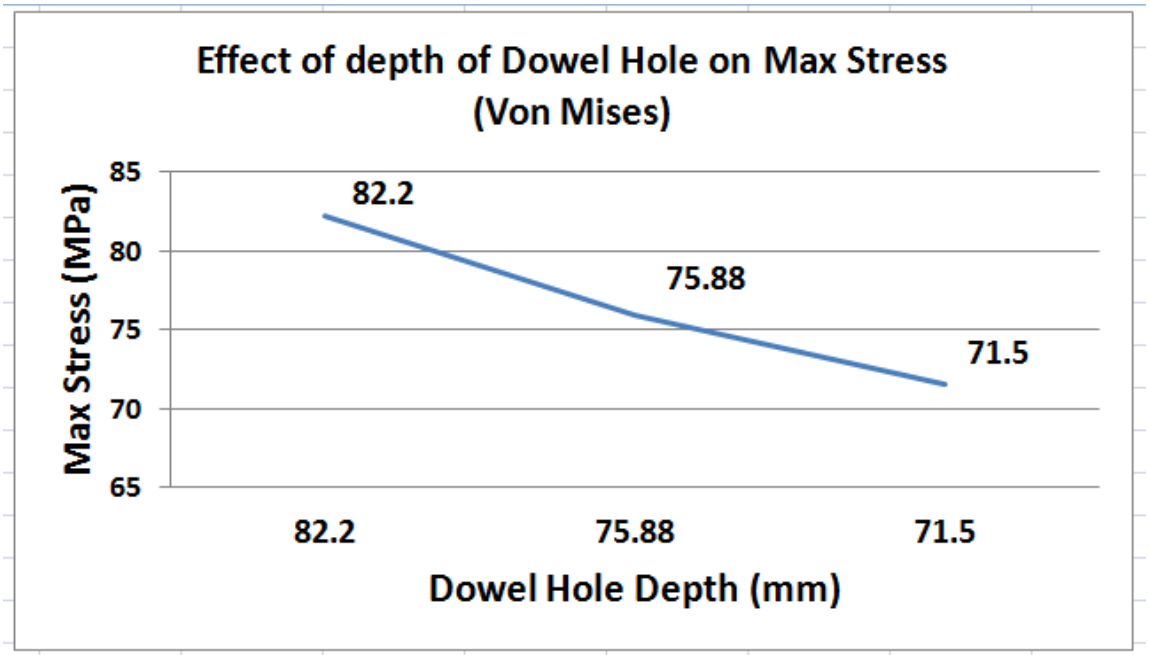

Fig 4.27: Plot showing variation in Max Stress (Von Mises) w.r.t. decrease in Dowel Hole Depth

4.4.4.3 Results:

1. It is observed that the decrease in depth of Dowel Hole in the flange is leading to reduction in the maximum stress level.
2. When compared with base model, it is seen that stress level is continuously coming down from a value of 82.1 MPa for the base model to a value of 71.5 MPa.
3. The maximum stress value is at the mouth of the dowel hole inside the flange. This indicates that the depth of the dowel hole is one of the most significant parameters in controlling the maximum stress values in the geometry under study.

4.4.5 EFFECT OF PROVIDING A VARIABLE RADIUS

It was considered as one of the alternatives to reduce maximum stress but considering the geometrical constraints of assembly, the option was found to be unviable. The reason is that there is no space for having higher root radius towards flange side. Therefore no further study was conducted on this option.

4.4.6 INCRESING THE PCD OF COUPLING HOLES

One more option was considered for study that was to increase the PCD of coupling holes to provide maximum metal condition near the stressed zone. This would have been done with reducing the size of coupling holes and corresponding increase in their numbers to compensate the shear strength.

But considering the location of the stressed zone, this option was dropped because highest level of stress is near the root and not near the coupling holes.

4.5 FINDINGS AND ANALYSIS OF FEA STUDIES

Four different geometric options have been tried for seeing their impact on the level of maximum stress induced by conducting FEA. The variations were subject to the manufacturing and assembly constraints in each geometric feature. These are :

1. Increase in the flange width – There is reduction in maximum stress but the there is marginal increase in the volume/weight of the component
2. Introducing a blended groove in the flange to increase root radius has not helped rather it increased the stress level.
3. Introducing a groove at the flange root in the shaft initially increased the stress level but with further increase, the stress level started reducing. Therefore as opposed to the groove in the flange, a groove in the shaft proved to be beneficial and reduced the stress level.
4. Lastly it is the depth of dowel hole, which has played most significantly to the objective of reducing the overall stress level. Reduction in the depth of dowel hole has reduced the notched zone in the stressed area therefore giving significant reduction in the maximum stress level.

4.6 DEVELOPMENT OF AN OPTIMISED MODEL BASED ON FEA STUDIES

Considering these results, a model was developed wherein all the favourable variations were combined to derive the optimised model in terms of lowest level of maximum induced stress.

Optimisation in this model is decided by the constraints imposed by machining and assembly constraints as has been done in earlier modelling. Therefore The following parameters were chosen for this optimised model;

1. Flange width increased from 18.26 mm to 26.99 mm.
2. Undercut of a radius of 3.05 mm introduced in the form a groove in the shaft.
3. The depth of the dowel hole is reduced to 7.62 mm.

With these geometrical features, a new 3-D model was developed using Creo Elements/Pro 5.0 as shown below.

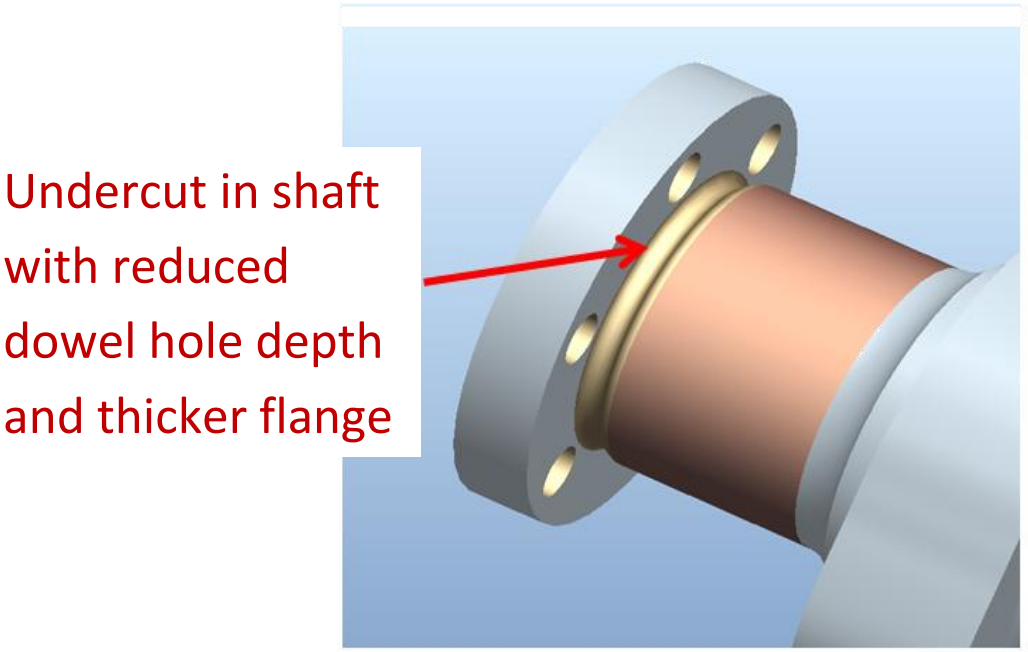

Fig 4.28 : Optimised 3-D Model with undercut radius of 3.05 mm, flange thickness of 26.99 mm & reduced depth of dowel hole of 7.62 mm

4.6.1 FEM ANALYSIS

The material being a ductile material at the flange root, primarily loaded with torque, therefore a shape distortion stress will be acting on it. In such a situation Von Mises Stress calculation is the most appropriate method to analyse the components for failure.

Though there will be various dynamic stresses on the camshaft during operation of the engine but most prominent stress will be caused by the torque transmission. By design calculations, it has been computed as

Max Torque T_{max} = 1996 Nm (2000 Nm)

For conducting FEA, the torque is simplified to an equivalent force acting on each of the six coupling holes.

The value of the force is calculated as

$$F_c = T_{max} / n X R$$

where n being number of coupling holes and

R being the pitch circle radius of coupling holes

$$F_c = 2000/ (6 X 90.5 X 10^{-3})$$

$$= 7.37 X 10^{3} N$$

Force F_c is applied tangentially at the PCD at all the six coupling holes on one flange and the surface of the opposite flange is considered as a fixed element to examine the effect of torque.

Weight of the finished component is about 23.2 Kg ~ 226 N

This force element on a rigidly supported member from both ends being considerably small compared to the forces acting because of torque has been ignored so as to make the model simple for study.

Solid models of SUCS has been prepared using the Creo Elements/Pro V.5.0 software. The Solid model has further been used for FEA meshing. Meshing has been done using Hypermesh v09 Software. FEM modelling has been done using Tetrahedral elements.. RADIOSS solver has been used for Linear Static Analysis.

Both 2D & 3D elemental stresses have been considered.

Size of the element : 2 mm

Number of elements : 553348 ~ 5.533 X 10^5

Number of nodes : 120656 ~ 1.206 X 10^5

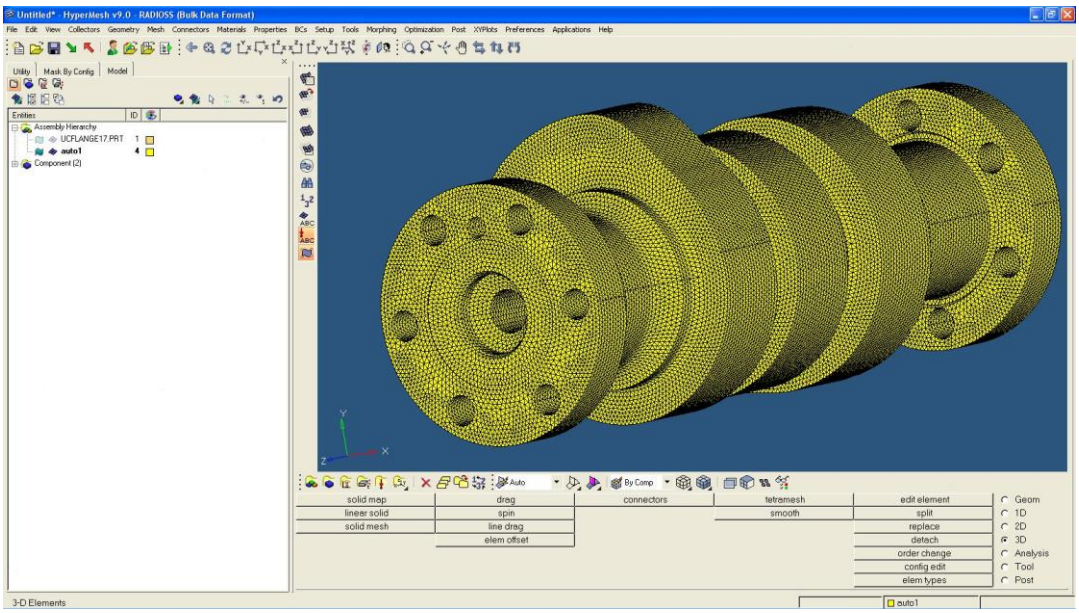

Fig 4.29 : Meshing done on Hypermesh v09 Software using Tetrahedral elements of 2mm size (with undercut in shaft, reduced dowel hole depth and thicker flange)

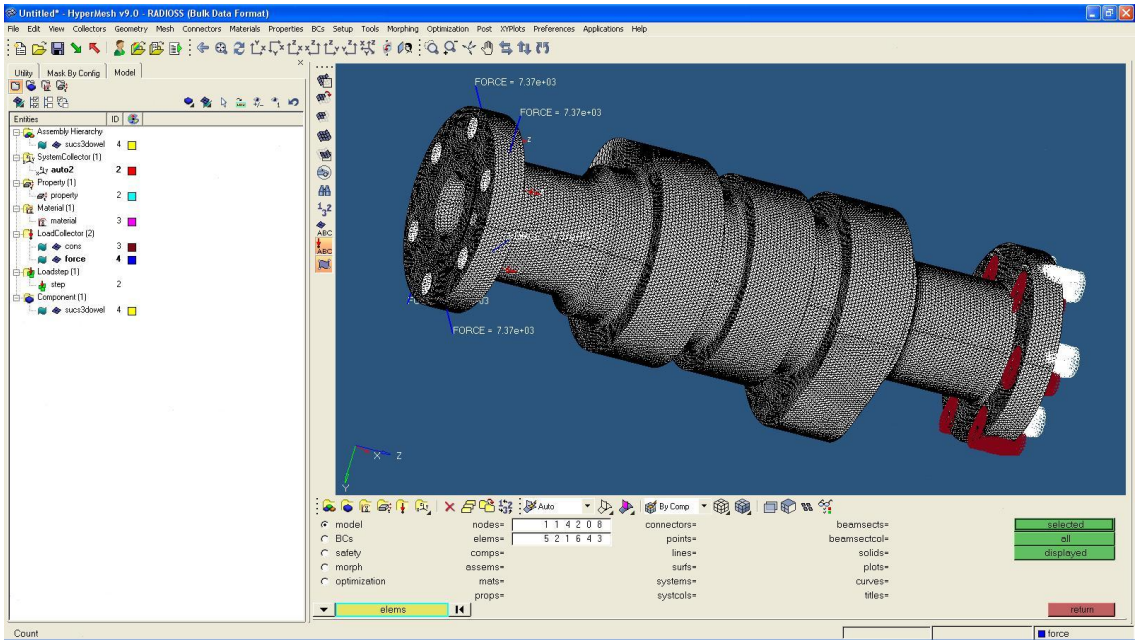

Fig 4.30 : Conversion of torque into equivalent force elements applied at PCD before FEA (with undercut in shaft, reduced dowel hole depth and thicker flange)

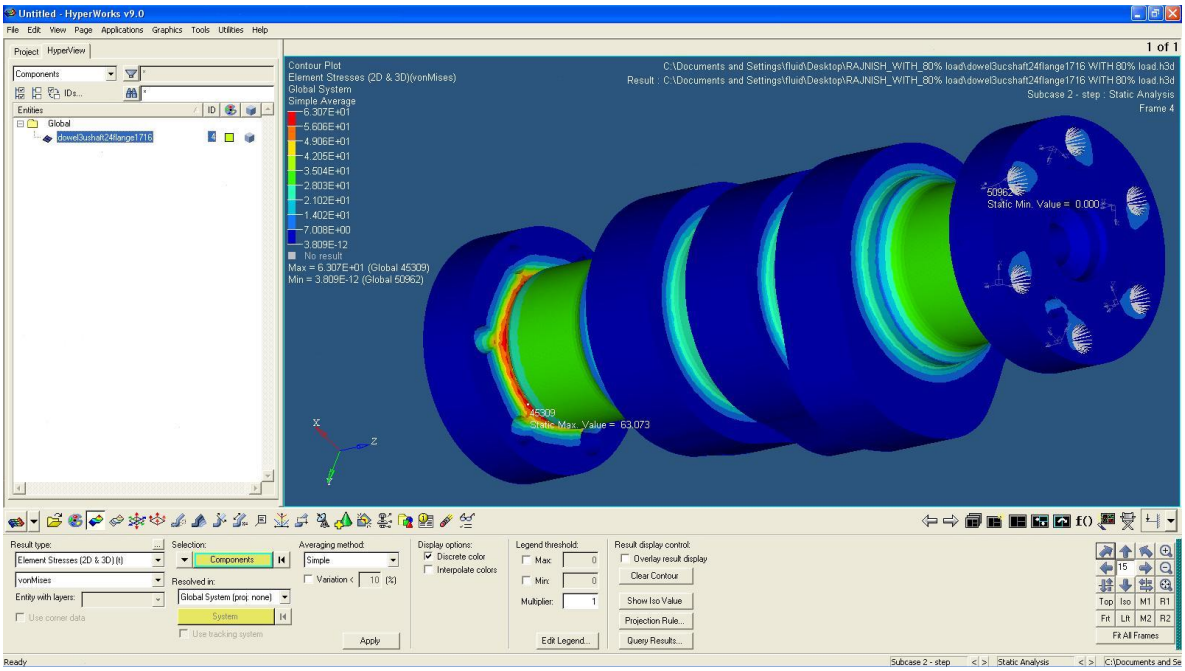

Fig 4.31 : FEA of the Optimised 3-D Model with undercut radius of 3.05 mm, flange thickness of 26.99 mm & reduced depth of dowel hole of 7.62 mm on RADIOSS solver

4.7 FINDINGS AND RESULTS:

It is observed that the decrease in depth of Dowel Hole combined with increased flange width and undercut groove in shaft is leading to reduction in the maximum stress level.

1. When compared with base model, it is seen that stress level is continuously coming down from a value of 91.7 MPa for the base model to a value of 63.7 MPa.
2. The maximum stress value is at the mouth of the dowel hole inside the flange. This indicates that the depth of the dowel hole is one of the most significant parameters in controlling the maximum stress values and reducing the SCF in the geometry under study.

Chapter 5

FORGING AS ALTERNATIVE MATERIAL FOR CAMSHAFTS

5.1 INTRODUCTION

Camshafts for small engines are normally manufactured by forging, but for large engines like locomotive and marine engines, rolled bars are the material of choice. The main reason is as that for large sized forgings (2-3 meter size), it is difficult to control the quality parameters and it also necessitates use of large dies and large presses. If the volume is not supportive, it becomes exorbitantly costly to go for forging.

Round bars on the other hands can be produced to any size by rollers of requisite size and the final size is achieved by machining. Thus raw material is relatively cheap and also material quality parameters are easy to control.

In the present situation, the existing camshaft design has been modified to make it sturdier so to withstand higher levels of fuel injection pressure. Being a retrofit design, the strengthening was achieved by increasing the base circle diameter of the camshaft. This design posed a constraint in assembly because bigger base circle dia couldn't be passed through the cam bores in the engine block. As a result, split design was developed as a viable method for assembly. Unit camshaft segments were the final solution which could be assembled in situ on the engine block without the need for them to pass through the cam bores. For coupling them together with each other and to the drive gear, spacers of lesser dia were designed, which could be accommodated within the existing cam bores of engine block.

This new design gave an opportunity to adopt forgings as an alternative to the rolled round bars for manufacturing of camshafts, because the design of each segment has been made identical and it has become much smaller for adoption to forging. This aspect was taken up in this study.

The advantages envisaged are;

1. Improved physical properties
2. Reduced consumption of raw material
3. Lower machining activity
4. Improved man-power productivity
5. Lower overall costs

Considering these multifarious advantages, a study was initiated on adoption of forging as the input material for manufacturing of camshafts.

5.2 CHOICE OF MATERIAL

The material used for rolled camshafts was equivalent to AISI E 1070 grade High Carbon Steel which is suitable for induction hardening of camshaft lobes. This material was selected by DMW after lot of experimentation, so initially the same grade material was adopted for forgings also. The Mechanical and Chemical properties for this material are tabulated below:

Mechanical Properties:

Table 5.1 : Mechanical Properties of Magnaflux Quality AISI E 1070 Grade Hot Rolled, Normalized and Tempered Steel suitable for Induction Hardening [20]

Sr.	Parameter	Specified Values
1	Tensile Strength (Min)	670 MPa
2	Yield Strength (Min)	350 MPa
3	% Age Elongation (Min)	17
4	% Age Reduction in Area (Min)	40
5	Hardness	190-230 BHN

Chemical Properties:

Table 5.2 : Chemical Properties of Magnaflux Quality AISI E 1070 Grade Hot Rolled, Normalized and Tempered Steel suitable for Induction Hardening [20]

Sr.	**Parameter**	**Specified Values (% age)**
1	Carbon	0.65 – 0.75
2	Phosphorus	0.3 Max
3	Sulphur	0.3 Max
4	Manganese	0.5-0.8
5	Chromium	0.15-0.30

Since the material has been found to be suitable for the application and no problem has been experienced in the past, so same material was adopted for forgings as well.

5.3 DEVELOPMENT OF FORGING PROCESS FOR CAMSHAFTS

Since, DMW was not having its own forging facility, so M/s Happy Forgings Ltd. Ludhiana, an industry leader in automobile forgings and also an existing supplier of Railways was identified as the vendor for development of forging process for the Stiffer Unit Camshafts.

After considering various aspects of the component geometry and operational requirement, a design was developed for the Dies to be used in the Die Forging Process. A simulation was run on **FORGE ® NxT Ver. 3.0** Software. The results of the simulation are shown in a tabulation;

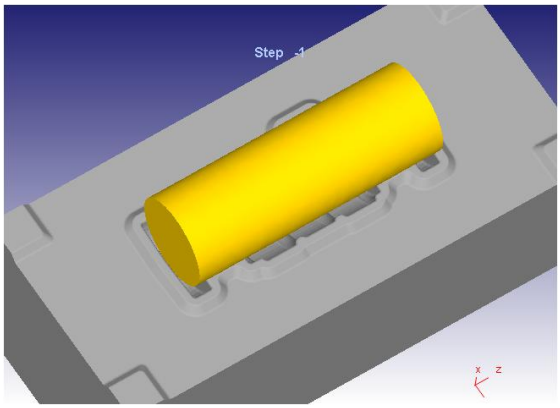

Step 1

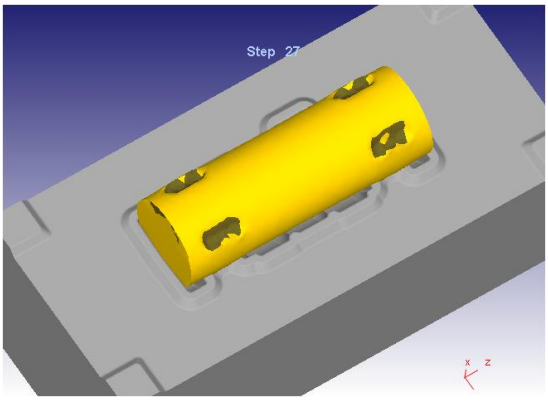

Step 27

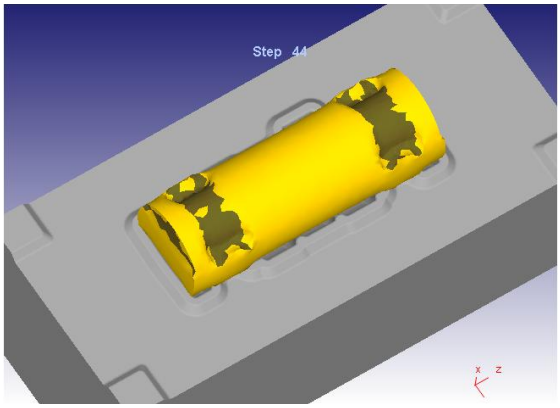

Step 44

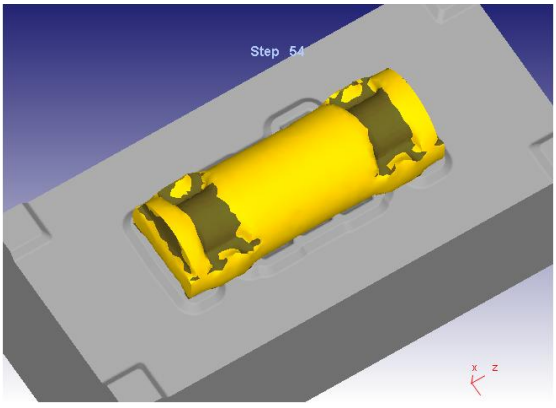

Step 54

…. figure continued

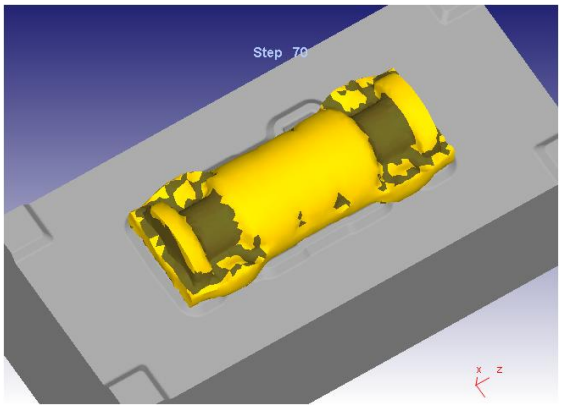

Step 70

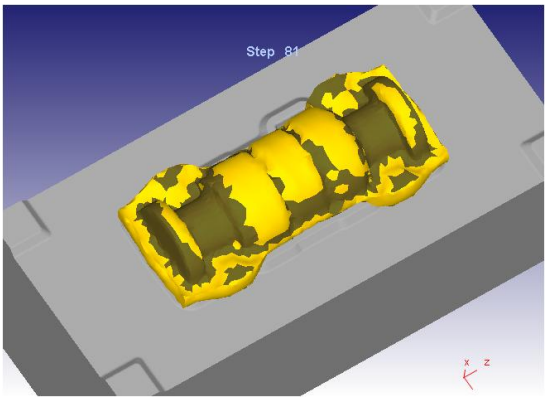

Step 81

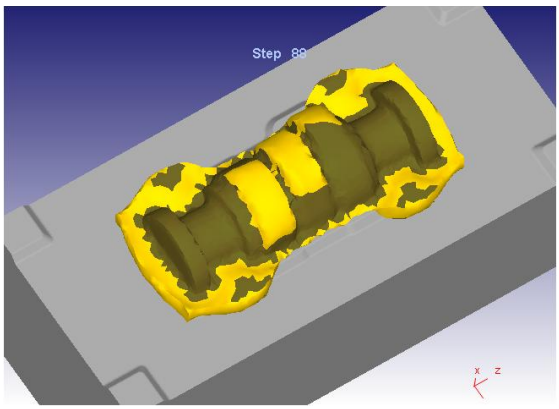

Step 89

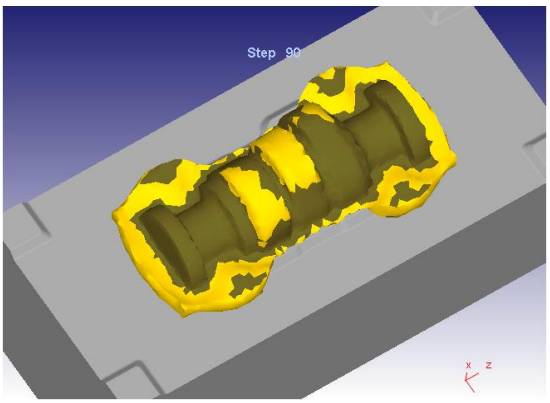

Step 90

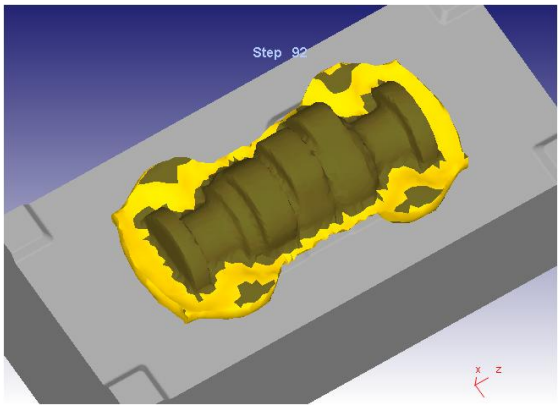

Step 92

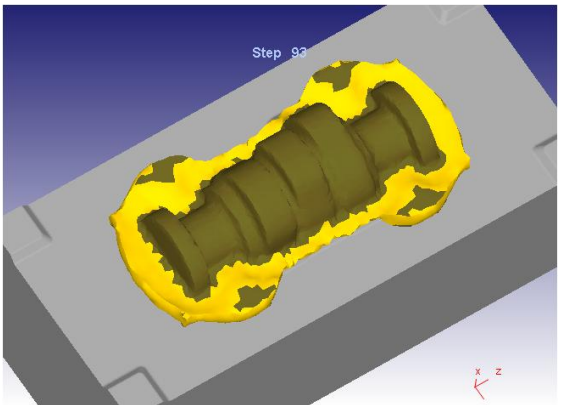

Step 93

Fig 5.1: Steps showing simulation of Stiffer Unit Camshaft Segment Die Forging, run on **FORGE ® NxT Ver. 3.0** Software [24]

After completing the simulation and validation of die design, Dies were developed and components were forged.

5.4 VALIDATION OF RESULTS

After adoption of forging process, the blanks of both round bar and forged component were examined for the following parameters.

5.4.1 METALLURGICAL EXAMINATION

The micro structure study revealed that the original structure containing distribution of Ferrite in Pearlite, Grain Size 6 was retained after forging with the exception that the grain size became finer conforming to ASTM grain size of 7. The examination was conducted on a Digital Microscope with 100 X magnification available in DMW Lab. The microstructure obtained is shown in the figure below. The finer structure is better for the application as it has the tendency to improve the strength of the material. It has further been seen that the physical properties of the material have also improved with the forging process.

Fig 5.2: Digital Microscope used for metallurgical examination [23]

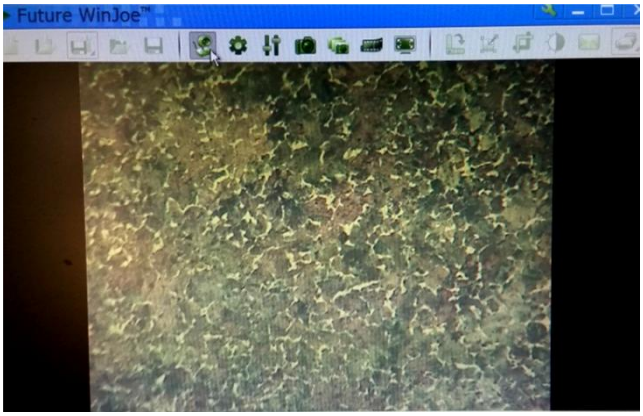

Microstructure of Round Bar –
AISI E 1070 Steel,
Distribution of Ferrite in Pearlite, Grain Size 6

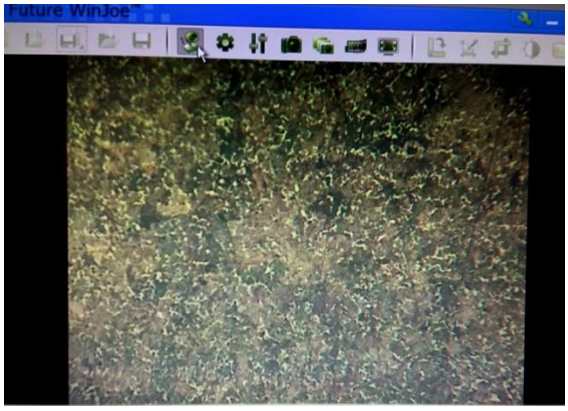

Microstructure of Forged Steel –
AISI E 1070 Steel, Distribution of Ferrite in Pearlite, ASTM Grain Size 7

Fig 5.3 : Comparison of Micro Structure (100 X)–grain refinement observed after forging [23]

5.4.2 ANALYSIS OF GRAIN FLOW AFTER FORGING

In order to analyse the grain flow, two pieces were cut from the middle and there section was cleaned with emery and etching so as to reveal the grain flow lines. Pictures shown below depict the grain flow lines in the cut section. It can be seen that the radius areas of flange roots have contoured lines which are definitely better than straight cut lines achieved in the rolled bars after turning operation is done.

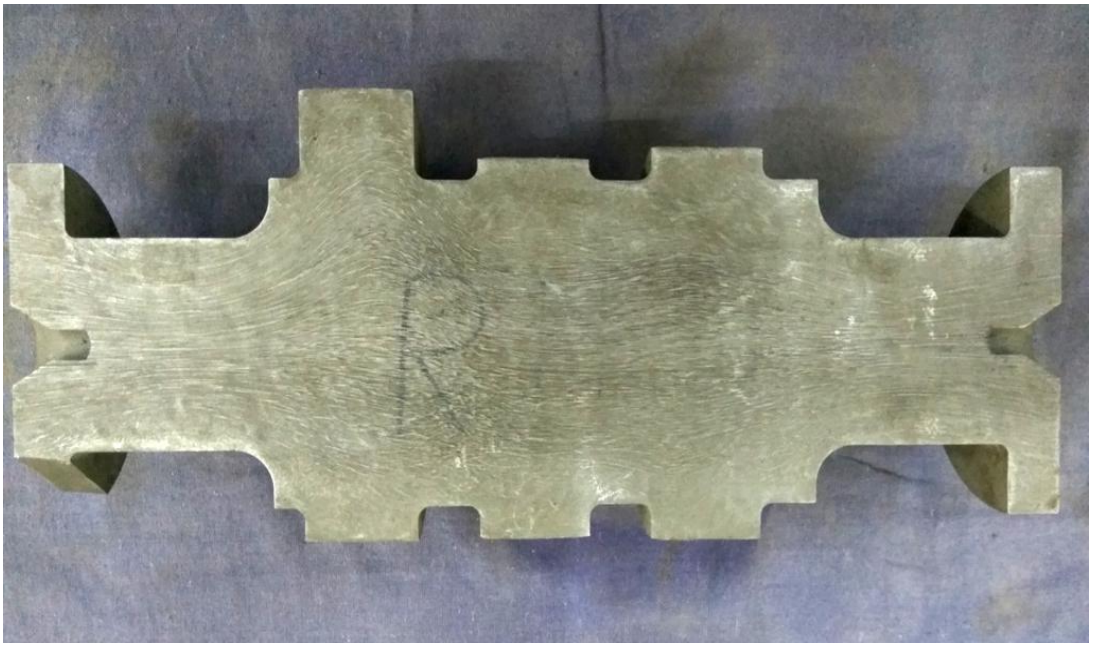

Sample -1

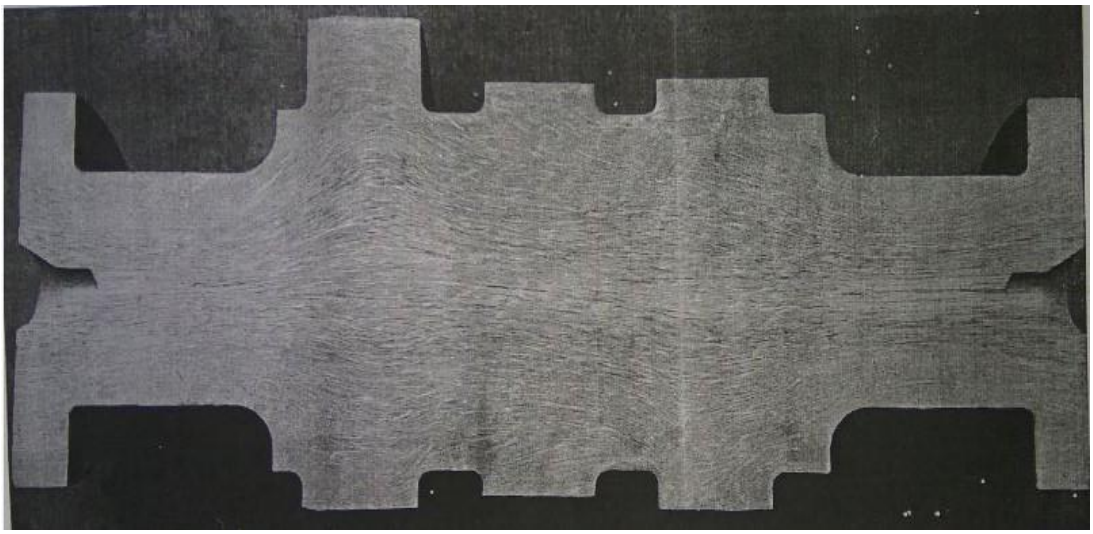

Sample -2

Fig 5.4 Grain flow lines as observed in a cut section of the forging [23]

5.4.3 STUDY OF PHYSICAL PROPERTIES

Further, the most important aspect of the study, i.e. improvement in physical properties, if any, were conducted in detail. During failure investigation of camshafts, it was revealed that the shear zone is concentrated near the flange roots due to stress concentration. Further the shear plane of failure existed at an aggle to the axis. So it needs to be seen that what kind of improvement has been achieved in the physical properties of material especially in that zone.

In order to study this aspect, following scheme was decided;

1. Five samples were prepared from the round bars for evaluating the mechanical properties of material along the grain flow.
2. Five more samples were prepared from the round bars for mechanical properties of material but across the grain flow.
3. As the failures have occurred at angle to the axis, thus five more samples were prepared especially at an angle of 45° to the axis.

These are shown in the figure shown below;

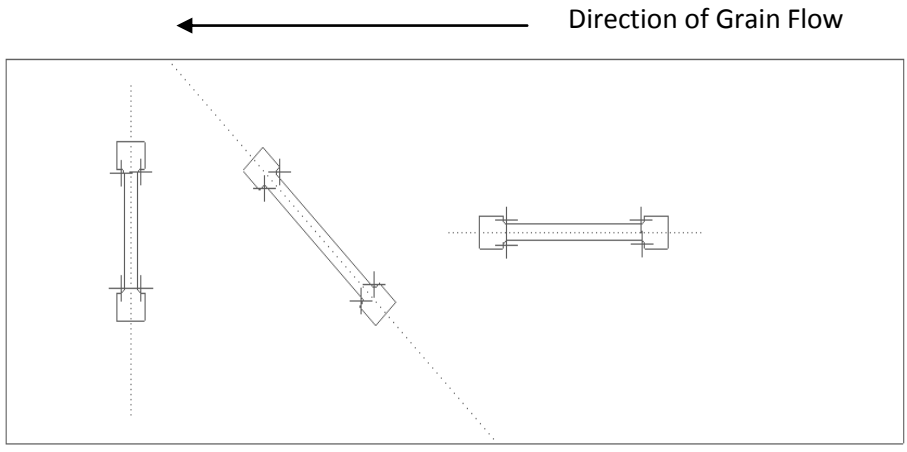

Fig 5.5 Scheme of samples prepared for study of Mechanical Properties in three different directions

Further, it is seen that in the forging, there are no grain flow lines in a particular section. So samples are drawn from the most vulnerable location as shown below in the fig 5.6;

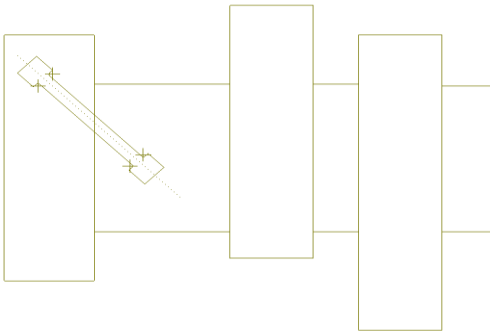

Fig 5.6 Location and alignment, from where sample is drwan for evaluating the Mechanical Properties of the Forging

Five more samples were prepared by cutting samples from the location shown above. These samples were tested on a Computerised Universal Testing Machine, Model TUE-C-400 available in the DMW Laboratory.

Fig 5.7 : Computerised Universal Testing Machine, Model TUE-C-400 available in the DMW Laboratory used for testing of Mechanical Properties of the samples [23]

5.4.3.1 Test Results

Test results obtained from the above mentioned tests are tabulated herein;

DIESEL LOCO MODERNISATION WORKS
C&M LABORATORY, DMW, PATIALA-147003

Machine Model	*TUE-C-400*	**Date:**	*17/10/16*
Machine Serial	*2011/109*	**Order #.**	*SUCS*
Customer	*CMT/LAB/DMW/Patiala*	**Lot No.**	*001*
Specimen Shape	*Solid Round*	**Test Type**	*tensile*
Material Type	*High Carbon Steel (AISI-E 1070)*	**Load Rate**	*0.33 kN/sec*
Specimen Description	*Round Bar (Along Grain Flow)*	**Strain**	*1.5*

Table 5.3: Mechanical Properties of Round Bar AISI E 1070 Steel (Along Grain Flow) [23]

TEST RESULTS

Sr	Parameter	Unit	S-1	S-2	S-3	S-4	S-5	Mean Values
1	Specimen Diameter	mm	9.2	9.9	9.5	9.4	10.0	
2	Initial Dist. between grips	mm	50.0	50.0	50.0	50.0	50.0	
3	Pre-Load Value	kN	0.0	0.0	0.0	0.0	0.0	
4	Max. Load	kN	400.0	400.0	400.0	400.0	400.0	
5	Max. Elongation	mm	200.0	200.0	200.0	200.0	200.0	
6	Specimen X -Section Area	mm^2	66.6	77.1	71.0	69.5	78.7	
7	Final Sp Diameter	mm	6.8	7.7	7.6	7.1	7.9	
8	Final Gauge Length	mm	60.7	59.2	58.4	60.1	58.6	
9	Final Area	mm^2	36.4	46.6	45.4	39.7	49.1	
10	Load at Yield	kN	32.0	31.3	31.2	32.2	32.0	
11	Elongation at Yield	mm	0.0	0.0	0.0	0.0	0.0	
12	Yield Stress	MPa	480.5	405.9	439.4	463.2	406.7	**439**
13	Load at Peak	kN	56.1	57.2	55.0	54.2	58.1	
14	Elongation at Peak	mm	7.8	6.3	5.6	7.3	5.5	
15	Tensile Strength	MPa	842.8	741.8	774.6	779.7	738.5	**776**
16	% Age Reduction in Area		45.37	39.51	36.00	42.95	37.59	**40.3**
17	% Age Elongation		21.4	18.4	16.8	20.2	17.2	**18.8**
18	Hardness	BHN	196	218	215	201	208	**208**

DIESEL LOCO MODERNISATION WORKS
C&M LABORATORY, DMW, PATIALA-147003

Machine Model	*TUE-C-400*	**Date:**	*19/10/16*
Machine Serial	*2011/109*	**Order #.**	*SUCS*
Customer	*CMT/LAB/DMW/Patiala*	**Lot No.**	*001*
Specimen Shape	*Solid Round*	**Test Type**	*tensile*
			0.33
Material Type	*High Carbon Steel (AISI-E 1070)*	**Load Rate**	*kN/sec*
Specimen Description	*Round Bar (Across Grain Flow)*	**Strain**	*1.5*

Table 5.4 : Mechanical Properties of Round Bar AISI E 1070 Steel (Across Grain Flow) [23]

TEST RESULTS

Sr	Parameter	Unit	S-1	S-2	S-3	S-4	S-5	Mean Values
1	Specimen Diameter	mm	9.9	9.3	9.8	9.6	9.2	
2	Initial Dist. between grips	mm	50.0	50.0	50.0	50.0	50.0	
3	Pre-Load Value	kN	0.0	0.0	0.0	0.0	0.0	
4	Max. Load	kN	400.0	400.0	400.0	400.0	400.0	
5	Max. Elongation	mm	200.0	200.0	200.0	200.0	200.0	
6	Specimen X-Section Area	mm^2	77.1	68.0	75.6	72.5	66.6	
7	Final Sp Diameter	mm	8.9	8.2	8.6	8.3	8.1	
8	Final Gauge Length	mm	55.1	55.9	55.6	57.2	56.1	
9	Final Area	mm^2	62.3	52.9	58.2	54.2	51.6	
10	Load at Yield	kN	24.5	24.6	23.9	24.8	25.0	
11	Elongation at Yield	mm	0.0	0.0	0.0	0.0	0.0	
12	Yield Stress	MPa	320	360	315	340	375	**345**
13	Load at Peak	kN	44.3	42.5	43.8	43.9	41.8	
14	Elongation at Peak	mm	5.5	7.3	6.3	5.6	7.8	
15	Tensile Strength	MPa	575	625	580	605	625	**600**
16	% Age Reduction in Area		19.18	22.26	22.99	25.25	22.48	**22.4**
17	% Age Elongation		10.2	11.8	11.2	14.4	12.2	**12.0**
18	Hardness	BHN	208	207	240	225	196	**215**

DIESEL LOCO MODERNISATION WORKS
C&M LABORATORY, DMW, PATIALA-147003

Machine Model	*TUE-C-400*	**Date:**	*19/10/16*
Machine Serial	*2011/109*	**Order No.**	*SUCS*
Customer	*CMT/LAB/DMW/Patiala*	**Lot No.**	*001*
Specimen Shape	*Solid Round*	**Test Type**	*tensile*
Material Type	*High Carbon Steel (AISI-E 1070)*	**Load Rate**	*0.33 kN/sec*
Specimen Description	*Round Bar (At 45°plane)*	**Strain**	*1.5*

Table 5.5 : Mechanical Properties of Round Bar AISI E 1070 Steel (At 45° plane) [23]

TEST RESULTS

Sr	Parameter	Unit	S-1	S-2	S-3	S-4	S-5	Mean Values
1	Specimen Diameter	mm	10.1	9.8	9.3	9.5	9.7	
2	Initial Dist. between grips	mm	50.0	50.0	50.0	50.0	50.0	
3	Pre-Load Value	kN	0.0	0.0	0.0	0.0	0.0	
4	Max. Load	kN	400.0	400.0	400.0	400.0	400.0	
5	Max. Elongation	mm	200.0	200.0	200.0	200.0	200.0	
6	Specimen X-Section Area	mm^2	80.3	75.6	68.0	71.0	74.0	
7	Final Sp Diameter	mm	8.8	8.0	8.1	8.0	7.8	
8	Final Gauge Length	mm	56.0	55.7	55.9	57.2	56.9	
9	Final Area	mm^2	60.9	50.4	51.6	50.4	47.9	
10	Load at Yield	kN	26.7	27.8	22.9	25.6	29.9	
11	Elongation at Yield	mm	0.0	0.0	0.0	0.0	0.0	
12	Yield Stress	MPa	330	370	335	360	405	**360**
13	Load at Peak	kN	50.7	49.8	42.7	47.1	53.1	
14	Elongation at Peak	mm	6.3	5.6	5.5	7.3	7.8	
15	Tensile Strength	MPa	630	660	625	660	715	**660**
16	% Age Reduction in Area		24.1	33.3	24.1	29.1	35.3	**29.2**
17	% Age Elongation		12	11.4	11.8	14.4	13.8	**12.7**
18	Hardness	BHN	239	213	208	207	198	**213**

DIESEL LOCO MODERNISATION WORKS
C&M LABORATORY, DMW, PATIALA-147003

Machine Model	*TUE-C-400*	**Date:**	*19/10/16*
Machine Serial	*2011/109*	**Order No.**	*SUCS*
Customer	*CMT/LAB/DMW/Patiala*	**Lot No.**	*001*
Specimen Shape	*Solid Round*	**Test Type**	*tensile*
Material Type	*High Carbon Steel (AISI-E 1070)*	**Load Rate**	*0.33 kN/sec*
Specimen Description	*Forging (At 45 °plane)*	**Strain**	*1.5*

Table 5.6 : Mechanical Properties of Forging AISI E 1070 Steel (At 45° plane) [23]

TEST RESULTS

Sr	Parameter	Unit	S-1	S-2	S-3	S-4	S-5	Mean Values
1	Specimen Diameter	mm	9.0	9.9	9.2	9.5	9.5	
2	Initial Dist. between grips	mm	50.0	50.0	50.0	50.0	50.0	
3	Pre-Load Value	kN	0.0	0.0	0.0	0.0	0.0	
4	Max. Load	kN	400.0	400.0	400.0	400.0	400.0	
5	Max. Elongation	mm	200.0	200.0	200.0	200.0	200.0	
6	Specimen X-Section Area	mm^2	63.9	77.1	66.6	71.0	71.0	
7	Final Sp Diameter	mm	7.3	8.1	7.8	8.0	7.5	
8	Final Gauge Length	mm	59.1	58.9	57.5	57.9	57.2	
9	Final Area	mm^2	41.9	51.6	47.9	50.4	44.3	
10	Load at Yield	kN	31.4	39.3	28.2	30.5	32.9	
11	Elongation at Yield	mm	0.0	0.0	0.0	0.0	0.0	
12	Yield Stress	MPa	490	510	425	430	465	**455**
13	Load at Peak	kN	52.2	68.2	51.5	55.4	57.7	
14	Elongation at Peak	mm	7.3	7.8	5.5	6.3	5.6	
15	Tensile Strength	MPa	815	885	775	780	815	**810**
16	% Age Reduction in Area		34.36	33.06	28.12	29.09	37.67	**32.0**
17	% Age Elongation		18.2	17.8	15	15.8	14.4	**15.8**
18	Hardness	BHN	211	234	208	241	251	**229**

5.4.4 Analysis of Results Obtained in Mechanical Testing:

The mean values of mechanical properties obtained in these tests can be summarised as follows;

Table 5.7 : Comparison of Mechanical Properties of Forged component over Round Bar at 45° shear plane

Parameter	**Lot-1**	**Lot-2**	**Lot-3**	**Lot-4**	**%age change over Round Bar**
Type of sample	**Round bar**	**Round bar**	**Round bar**	**Forging**	
	Along grain flow	*Across grain flow*	*At 45 °plane*	*At 45 °plane*	*at 45 °plane*
UTS (MPa)	775	600	660	810	+22.73 (Over Lot-3)
Yield Strength (MPa)	440	345	360	455	+26.39 (Over Lot-3)
Elongation (%)	18.8	12.0	12.7	15.8	-15.9% (Over Lot-1)
Reduction in Area (%)	40.3	22.4	29.2	32.0	-20.6% (Over Lot-1)
Hardness (HB)	208	215	213	229	+7.51 (Over Lot-3)

Test Specimen taken from forging showing reduction in X-section area at the point of breakage

A cup and cone type breakage recorded during tensile test

Fig 5.8 : One of the test specimen showing cup and cone type breakage

The mechanical properties recorded during tests could also be noticed in the type of fracture that occurred during elongation tests. Due to work hardening during forging, the grain structure got refined and it improved the physical properties of the material

with corresponding reduction in ductility as can be visualized in the Reduction in Area and Elongation values.

But the substantial improvement in UTS and Yield values to the tune of 22.73% and 26.39%, attributable to the work hardening and better aligned grain flow lines is significant achievement in improving the fatigue life of the component.

5.5 RELATIVE ECONOMICS OF ADOPTING FORGING OVER ROLLED BARS

A study was conducted to see, what is the impact of adopting forgings over round bars. DMW decided to procure the forged Stiffer Unit Camshafts blanks in proof machined stage as shown in the picture below.

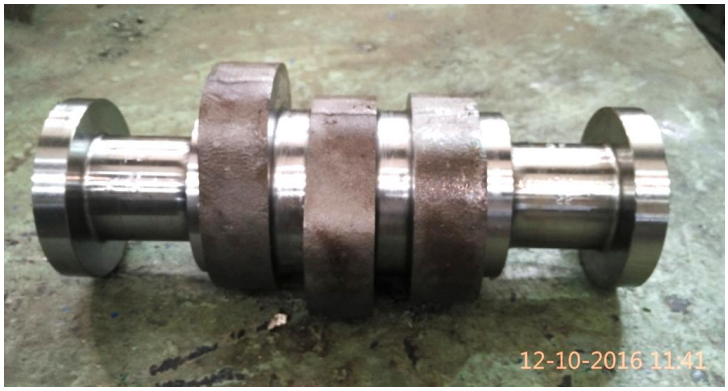

Fig 5.9: A proof machined forging adopted for manufacturing of Stiffer Unit Camshafts

This adoption resulted in lot of changes in the manufacturing process. Many machining steps were eliminated from the manufacturing process. The most prominent being the massive turning operation in which 160 mm round bar was being reduced to about 100 mm dia near the flanges.

Table 5.8: A comparison of stock removed in machining in the two processes

Sr	**Type**	**Round Bar**	**Forging**
1	Weight of raw material	64.0 kg.	29.5 kg
2	Weight of finished component	21.4 kg.	21.4 kg
3	**Amount of stock removed in machining**	**32.6 kg**	**08.1 kg**

It can be seen that amount of material removed during machining has seen a major change as only 8.1 kg material is removed against 32.6 kg in the earlier process, a reduction of 75% is achieved.

It also needs to be seen that though there is substantial reduction in the material removed during machining, but number of stages of machining has not undergone any major change. A detailed step by step time study indicated that the time taken for all machining and heat treatment processes has come down from 17.06 hrs. to 9.21 hrs. Further, developing a die set is a mojor investment in the forging process which is amortized over a long period depending on the volume of production. In the present situation DMW has demand for about 1000 sets of camshafts per year which amounts to 8000 nos. each of LHS and RHS segments. Considering this volume over an expected life of 20,000 strokes, the forging vendor has quoted a rate based on which cost comparison has been made. A tabulation below shows the net impact it has given on the cost of the component.

Table 5.9 : Table showing cost comparison of the two processes; Round Bar Vs Forging

Sr	**Cost Elements**	**From 160mm Round Bar** (PL # 90726420)	**From Proof machined Forgings** (RHS:10142782 & LHS:10142794)
1	Raw Material Cost	64 kgs X Rs. 59.20/kg = Rs. 3978	Per segment = Rs. 5846
2	Machining (Labour) Cost @ Rs.208/hr	17.06 hrs. X Rs. 208/hr = Rs. 3548	9.21 hrs. X Rs.208/hr = Rs. 1916
3	Overheads @ 216.33% of Labour cost	Rs. 3548 X 2.1633 = Rs. 7678	Rs. 1916 X2.1633 = Rs. 4157
	Total Cost /segment	**Rs. 15205**	**Rs. 11919**

Savings in cost per segment: Rs. 15205 – Rs. 11919 = Rs. 3286. (21% reduction) (20)

So from the above study, it is revealed that for a volume of 16000 segments per year, it amounts to a saving of Rs. 5.25 Crs. Per Annum.

5.6 FINDINGS & RESULTS

From this study, it has been seen that by adopting forging process for manufacturing of camshaft segments, the material properties could be improved by 22% in UTS and about 26% in Yield Strength at the vulnerable location.

This improvement is mainly attributable to the right kind of alignment of grain flow during forging as well as work hardening that simultaneously happens during the forging process.

Further, due to reduction in the amount of material to be removed by machining, the overall cost of manufacturing has come down by about 21% for a given volume of about 8000 nos. per annum.

Chapter 6

FINDINGS AND CONCLUSION

6.1 FINDINGS

The study pertained to identifying the reasons for failures occurring in the camshafts used in high horse power diesel locomotive engines. After analysing the reasons for failures, the task at hand was to find an optimal technical solution to the problem and summarize the findings and conclude the results which can be applied for similar applications elsewhere by design and production engineers.

Detailed analysis of the failures led to the findings that failures are occurring because of fatigue mainly caused by higher level of Stress Concentration Factor in the failure zone. The component geometry needed modification to reduce the stress level. Since the geometry was constrained by many manufacturing and assembly constraints, so there was limited play in the design to incorporate any change in the shape and size of geometrical features. Within these constraints different options were tried to find an optimal solution.

In this milieu, the study has been conducted in two parts, viz.

1. Incorporating changes in size and shape of the geometrical features for reduced stress concentration factor.
2. To incorporate change in the manufacturing process by adopting forgings instead of rolled bars for manufacturing of camshafts.

From the first part of study involving 3-D modelling and FE Analysis, it has been found that certain changes can be incorporated in the geometry of components which can reduce the stress concentration factor considerably. These changes are particularly useful for the components used in transmission of torque through flanged couplings in tight space constraints;

1. An undercut groove on the shaft diameter, blended with the flange face results in reduction of maximum level of stress induced.
2. On the other hand, an undercut groove in flange, blended with the shaft dia. results in increase in the maximum level of stress.
3. Increased flange thicknesses can be used to reduce the stress level to a limited extent as it will lead to increase in the weight of the component.

4. The most useful finding from this study has been a revelation that the depth of the dowel hole plays a significant role in increasing the SCF because of sudden change in x-section brought in by these holes on the flanges. The earlier studies on dowel holes had remained confined to the type of fits to be used for dowel pins in the two mating parts, but no study is available which focuses on the length of dowels to be used. In this study, it has been found that reducing the depth of dowel holes in the flanges has most significant role to play in bringing down the SCF. It has least impact on the weight of the component but can significantly increase the resistance to fatigue failures.

5. The other option initially considered for trial i.e. introducing variable radius, was found to unfeasible for implementation so it was dropped.

   Based on the results obtained by geometrical modelling and FE Analysis a combination model was developed to incorporate all the beneficial features together with boundary conditions, it was found that max. stress level could be reduced from 91.7 MPa to 63.7 MPa, thus showing an improvement of 30.5% in the SCF. This has the potential to increase the fatigue life of the component by at least 10 times from and existing level of 10^8 cycles to 10^9 cycles. With this the failures occurring prematurely can be very well controlled and full service life of 6 years can be obtained in the camshafts without any chance of fatigue failure during service.

The 2nd part of the study pertained to adoption of forgings in place of rolled bars for AISI E 1070 grade steel used in manufacturing. For conducting experimental studies, dies were designed and developed for the forging. While designing of the dies, it was kept in mind that the grain flow lines should remain perpendicular to the plane of failure so as to get maximum strength of the material.

Samples were drawn from the round bars in three different directions viz. along the grain flow, across the grain flow and at 45 deg plane which is perpendicular to the plane of failure. Similar sample was drawn from the forging for a comparison. It was revealed that after adopting forging process, there is marked improvement in the UTS and Yield Stress across the 45 deg plane. An improvement of 22% in UTS and 26% in

Yield Strength was achieved in these experiments. These improvements are attributable to right direction of grain flow at the shear plane and also due to work hardening during forging process as has been observed in the microstructure analysis.

6.2 CONCLUSION

From this study it has been concluded that by incorporating certain geometrical features in the geometries, the SCF can be significantly improved which in turn help in increasing the fatigue life of torque transmitting components. It is further concluded that adopting forging instead of rolled bars for manufacturing of camshafts, the material strength can be improved considerably that can help increase the strength of the material at vulnerable locations to withstand higher level of stresses.

6.3 SCOPE FOR FURTHER STUDY

As has been found in this study that certain geometrical features have significant impact in improving the SCF in cyclically loaded components, other standard geometric features used in machine components like threaded holes, threaded flanges, knuckles, locking pins etc. can be studied and their impact can be seen on the SCF for guiding the design engineers while development of new designs

Similarly many other components manufactured out of rolled bars and prone to failures like axles, shafts, lead screws, ball screws etc. can be examined for their failures during service and carefully designed forgings can be developed for better grain flow at the plane of failures.

These studies will find lot of potential for field application in improving the service life of the cyclically loaded components and may also reduce their cost of manufacturing.

REFERENCES

1. B. Boardman. Fatigue Resistance of Steels. ASM Handbook, Volume 1: Properties and Selection: Irons, Steels, and High-Performance Alloys (1990) 673-688.
2. A.I. Mourad, A. El-Domiaty, Y.J. Chao. Fracture Toughness Prediction of Low Alloy Steel as a Function of Specimen Notch Root Radius and Size Constraints. Engineering Fracture Mechanics 103 (2013) 79-93.
3. D. Taylor, A. Kelly, M. Toso, L. Susmel. The Variable-Radius Notch: Two New Methods for Reducing Stress Concentration. Engineering Failure Analysis 18 (2011) 1009-1017.
4. G. Cevik, R. Gurbuz. Evaluation of Fatigue Performance of a Fillet Rolled Diesel Engine Crankshaft. Engineering Failure Analysis 27 (2013) 250–261.
5. C.S. Bandara, S.C. Siriwardane, U.I. Dissanayake, R. Dissanayake. Fatigue Failure Predictions for Steels in the Very High Cycle Region – A Review and Recommendations. Engineering Failure Analysis 45 (2014) 421-435.
6. F.J. Espadafor, J.B. Villanueva, M.T. García. Analysis of a Diesel Generator Crankshaft Failure. Engineering Failure Analysis 16 (2009) 2333–2341.
7. R. Avilés, J. Albizuri, E. Ukar, A. Lamikiz, A. Avilés. Influence of Laser Polishing in an Inert Atmosphere on the High Cycle Fatigue Strength of AISI 1045 Steel. International Journal of Fatigue 68 (2014) 67–79.
8. A. Wormsen, M. Avice, A. Fjeldstad, L. Reinås, K. A. Macdonald, A. D. Muff. Base Material Fatigue Data for Low Alloy Forged Steels Used in the Subsea Industry. Part 1: In Air S–N Data. International Journal of Fatigue 80 (2015) 477–495.
9. Z. Yu, X. Xu. Failure Investigation of a Truck Diesel Engine Gear Train Consisting of Crankshaft and Camshaft Gears. Engineering Failure Analysis 17 (2010) 537–545.
10. H. Bayrakceken, I. Ucun, S. Tasgetiren. Fracture Analysis of a Camshaft Made from Nodular Cast Iron. Engineering Failure Analysis 13 (2006) 1240–1245.
11. A Report: Upgradation of ALCO Locomotive Engine Design - The In-House Effort by Indian Railways. Downloaded from http://www.irimee.indianrailways.gov.in/instt/uploads/files/1434534063426-Upgradation%20of%20ALCO%20loco%20design.pdf on 15.11.2015

12. J. P. Fuertes, C. J. Luis, R. Luri, D. Salcedo, J. Leon, I. Puertas. Design, Simulation and Manufacturing of a Connecting Rod from Ultra-fine Grained Material and Iso-thermal Forging. Journal of Manufacturing Processes 21 (2016) 56-68.
13. L. Fan, Z.Wang, He Wang. 3D Finite Element Modelling and Analysis of Radial Forging Process. Journal of Manufacturing Processes 16 (2014) 329-334.
14. Y. H. Zhang, S. J. Maddox, S. Manteghi. Verification of Class B S-N Curve for Fatigue Design of Steel Forgings. International Journal of Fatigue 92 Part-1 (2016) 246-261.
15. A. Wormsen, M. Advice, A. Fjeldstad,, L. Reinas, K. A. Macdonald, A. D. Muff. Base Material Fatigue Data for Low Alloy Forged Steels used in the Subsea Industry Part-1: In Air S-N Data. International Journal of Fatigue 80 (2015) 477-495.
16. M. Decker, M. Eiber, S. Rodling. Challenges in the Fatigue Assessment of Large Components from Forged or Cast Iron. Procedia Engineering 133 (2015) 726-735.
17. P. Bereczki, V. Szombathelyi, G. Krallics. Determination of Flow Curve at Large Cyclic Plastic Strain by Multiaxial Forging on MaxStrain System. International Journal of Mechanical Sciences 84 (2014) 182-188.
18. J. Herrmann, T. Rauert, P. Dalhoff, M. Sander. Fatigue and Fracture Mechanical Behaviour of a Wind Turbine Rotor Shaft Made of Cast Iron and Forged Steel. Procedia Structural Integrity 2 (2016) 2951-2958.
19. A. Yapici, G. Saracoglu. Fatigue Analysis of Bolted Flange Joints of a Rotary Dryer. Engineering Failure Analysis 63 (2016) 182-190.
20. Loco Design Office, Diesel Loco Modernisation Works, Patiala.
21. Quality Assurance Dept., Diesel Loco Modernisation Works, Patiala.
22. Centre for Excellence in Design, Rail Coach Factory, Kapurthala.
23. C&M Lab, Diesel Loco Modernisation Works, Patiala.
24. M/s Happy Forgings Ltd., Ludhiana.